CHITOSAN AND PEGYLATED CHITOSAN NANOPARTICLES FOR FUNCTIONAL GENE SILENCING IN COLORECTAL CANCER CELLS

by

Abuzar Ahmed, B.E.

A thesis submitted to the Graduate Council of
Texas State University in partial fulfillment
of the requirements for the degree of
Master of Science
with a Major in Biochemistry
December 2013

Committee Members:

Walter E. Rudzinski, Chair

Michelle A. Lane

Tania Betancourt

FAIR USE AND AUTHOR'S PERMISSION STATEMENT

Fair Use

Duplication Permission

DEDICATION

I dedicate my thesis work to my family. A special feeling of gratitude to my loving parents, Marzia Saud and Saud Ahmed for always being there for me and whose words of encouragement made me achieve my goals. My brother, Faizan Ahmed has been my strength and his support has always been very special to me.

ACKNOWLEDGEMENTS

First I would like to acknowledge my Committee chair Dr. Walter E. Rudzinski for believing in me and providing me with a research opportunity in his lab. Secondly I would like to acknowledge my committee members Dr. Michelle A. Lane and Dr. Tania Betancourt for their guidance, support and time with my thesis. Thirdly I would like to acknowledge the professors for granting me access to their labs to use their equipment and helping me with their expertise in analyzing the results: Dr. Kevin Lewis, Dr. Ron Walter and Dr. Dana Garcia. I would like to acknowledge Dr. Todd W. Hudnall for training me on the NMR equipment. I would like to acknowledge Mrs. Alissa Savage and Mr. Eric Schires for their time and effort to train me and helping me work on instruments. I would like to thank the Department of Chemistry and Biochemistry (Texas State) for accepting me into their program and giving me and opportunity to learn from the best brains in the industry. I would like to acknowledge Dr. Chad Booth for his encouragement and support. Lastly I would like to acknowledge the members in my lab group: Mrs. Adriana Soliz Palacios, Mr. Edgar Vargas and Mr. Shachindra Nargund for their support.

TABLE OF CONTENTS

Page

LIST OF TABLES

Table **Page**

LIST OF FIGURES

Figure **Page**

ABSTRACT

RNA interference (RNAi) technology is a useful mechanism for inhibiting gene expression. This technology involves the use of small interfering RNA (siRNA) for gene therapy purposes. We have made an effort to use this technology to reduce the expression of beta-catenin in colon cancer cells. The pharmaceutical application of siRNA is dependent on an efficient delivery system. The positively charged nature of chitosan provides interesting properties with respect to interaction with oppositely charged materials, especially those of high molecular weight. Interaction between positively charged chitosan and negatively charged siRNA can be exploited; making chitosan an ideal candidate to serve as a delivery vehicle for siRNA. The most important problem associated with the use of chitosan is its limited solubility at pH higher than its pKa (5.5-6.5). Being a weak base chitosan is only completely soluble under acidic conditions. To overcome the problem of solubility we have grafted poly (ethylene glycol) to chitosan. PEGylated chitosan/siRNA and chitosan/siRNA nanoparticles have been synthesized and characterized. Size characterization of nanoparticles was carried out using transmission electron microscopy (TEM), scanning electron microscopy (SEM) and dynamic light scattering (DLS) techniques. The encapsulation efficiency was evaluated using a nanodrop (UV absorption detector). HCT 116 colorectal cancer cell line was used to evaluate the transfection of siRNA across the cellular membrane. The cell lines were treated with 0.1 and 0.5 nmol of siRNA encapsulated in PEGylated chitosan and chitosan for a period of 24 and 48 hours. The percent reduction in beta-catenin protein level was

evaluated using the western blot technique. The chitosan/siRNA and PEGylated chitosan/siRNA nanoparticle approach was compared to the classical approach used for siRNA delivery; namely siRNA in Lipofectamine 2000 to identify the difference in the levels of beta-catenin protein in HCT 116 cells. We were successful in reducing the cellular beta-catenin protein levels and both the chitosan/siRNA and PEGylated chitosan/siRNA approaches were successful in reducing beta catenin protein levels after 48 h. Another significant result was that the chitosan/siRNA had a similar ability as Lipofectamine/siRNA to reduce beta catenin protein levels when administered at a sufficient concentration of siRNA.

.

CHAPTER I

INTRODUCTION

1.1 Colon Cancer

Colon cancer also known as colorectal cancer initiates in the large intestine or the rectum. According to the American Cancer Society and the National Cancer Institute (NCI), colon cancer is the third most common cancer behind lung and breast cancer (Siegel et al., 2013). If the cancer is detected during early stages; surgery remains as the only option of definitive treatment and the chances of survival are between 80-95% (Goldstein et al., 2005). Unfortunately the chances of survival in the advanced stages are reduced to 10-30% (Goldstein et al., 2005). Almost all colon cancer initiates in the glands lining the colon and rectum. Our research focusses on reducing the increased level of beta-catenin that occurs with colon cancer.

1.2 The Role of beta-catenin in Colon Cancer

Beta-catenin is part of a complex of proteins that constitute adheren junctions. Adheren junctions or zonula adheren are essential elements required for establishing cell-cell contacts and are important in the maintenance of the integrity of the epithelial layers (Figure 1). In normal cells, beta-catenin functions as a component of the adheren complex by binding with E-cadherin. Beta-catenin is also responsible for regulating cell growth and adhesion between cells. Beta-catenin is an essential member of the Wingless-Wnt signal transduction pathway. In the Wnt signal transduction pathway, beta-catenin aids in transducing the Wnt signal from the cell surface to the nucleus. At the cell surface reception of the Wnt signal results in the stabilization of beta-catenin, followed by

accumulation of beta-catenin in the nuclei. The interaction of beta-catenin with the LEF/TCF binding proteins activates transcription of the Wnt responsive genes (Cavallo et al., 1997). In the absence of the Wnt signaling, the cytoplasmic beta-catenin degrades and only membrane bound beta-catenin complexed with cadherins is protected from degradation. Beta-catenin levels rise upon the reception of the Wnt signal, due to stabilization against proteolysis of uncomplexed beta-catenin in the cell (Papkoff et al., 1996).

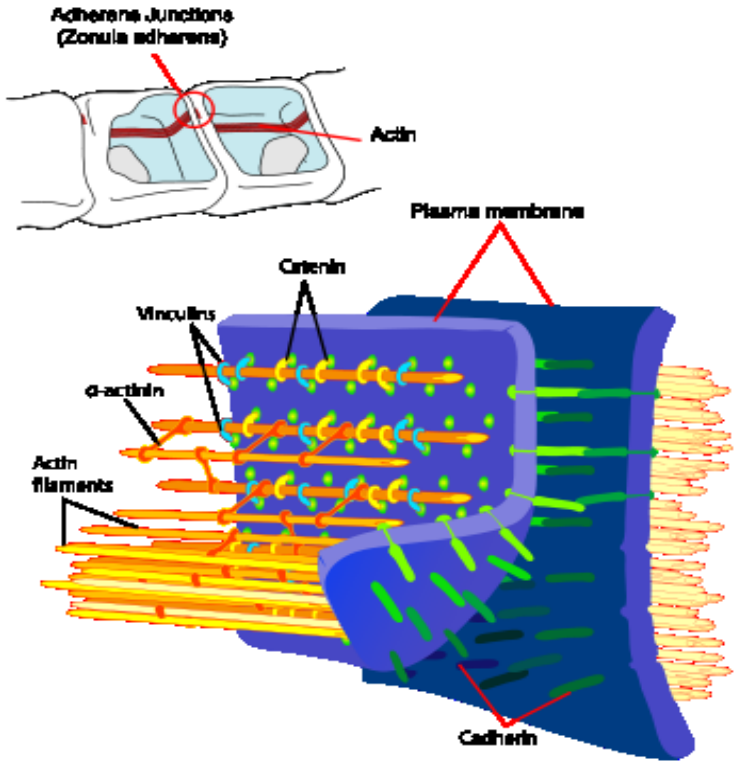

Figure 1. Adheren junction.

The mechanism used by the Wnt signal to increase the level of beta-catenin is not clear but research using Drosophila (Pai et al., 1997; Peifer et al., 1994) and Xenopus (He et al., 1995; Yost et al., 1996) have suggested that Zeste-white 3 kinase/Glycogen synthase kinase 3 (ZW-3/GSK-3) is involved in the degradation of beta-catenin. Studies have also shown that phosphorylation of beta-catenin is the most likely mechanism for the regulation of its degradation (Daniel and Reynolds, 1997). In mammals, the GSK-3 functions in tandem with the adenomaceous polyposis coli (APC) and Axin to regulate the degradation of beta-catenin by the ubiquitin-proteasome system and restricts the beta-catenin level in the cytoplasm (Sandra et al., 1999). Regulation of beta-catenin levels in the transduction of the Wnt-signal is a key factor; this is because increased levels of beta-catenin are found in 70-80% of colon tumors, due to mutations in the APC gene. In the event of mutation of APC gene, beta-catenin moves into the cell nucleus. The interaction of beta-catenin with the TCF/LEF family of transcription factors induces gene expression that stimulates tumor cell proliferation (Li et al., 2005).

1.3 RNA Interference

RNA Interference or (RNAi) was discovered in 1998 by Andrew Fire and Craig Mello in the nematode worm Caenorhabditis elegans (Fire A et al., 1998) and later found in a variety of organisms, including mammals. RNAi is a potent and highly specific gene-silencing phenomenon triggered by double stranded RNA helices (Couzin et al., 2002). In the RNA interference process, the introduction of 21-23 base pair small interfering RNA, called siRNA in cells results in the degradation of homologous mRNA and specific protein knock down. The gene silencing property of siRNA is not unusual, since scientists and researchers have been silencing genes using single stranded antisense-

oligodeoxyribonucleotides (ASO) (Pack et al., 2005; Akhtar et al., 2007; Aagaard, L and Rossi, J. 2007). The success of RNAi as a remedy depends upon the effective knockdown of targets and efficient intracellular delivery of siRNA. The RNAi mechanism is shown in Figure 2.

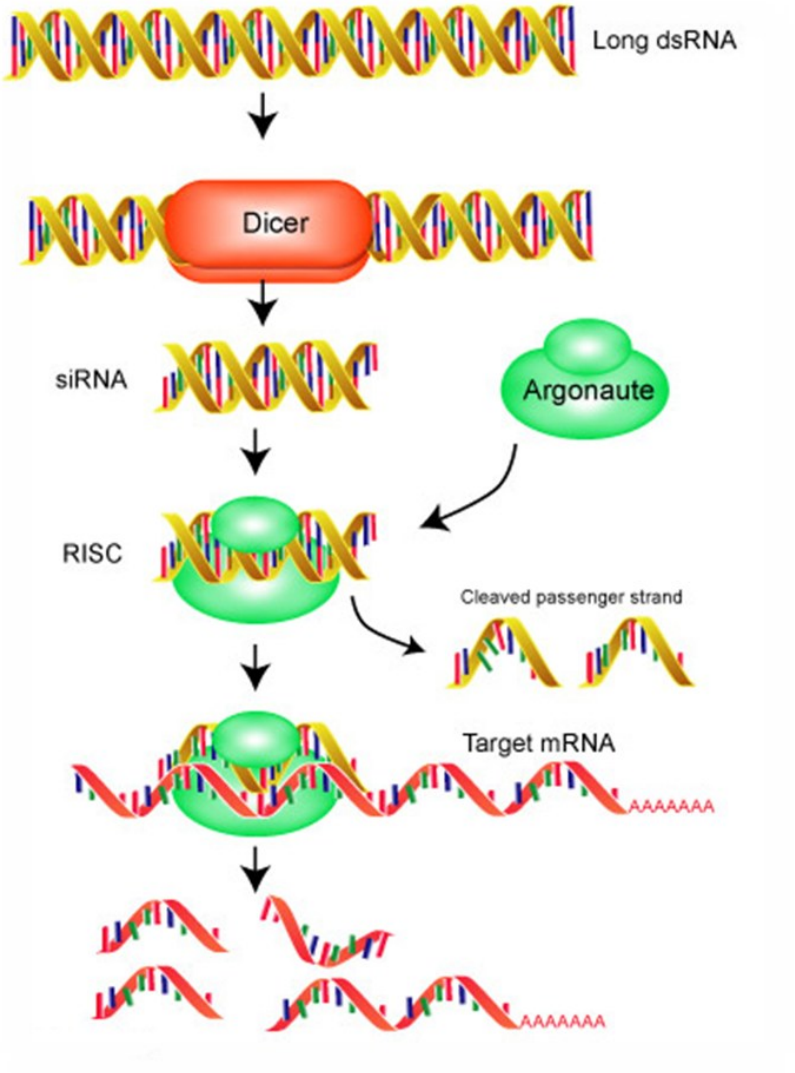

Figure 2: RNAi mechanism

The RNA interference process is initiated by long double-stranded (ds) RNA helices. These dsRNA are first processed by a ribonuclease III enzyme called as Dicer, into a 21-23 nucleotide (nt) small interfering RNA (siRNA). The siRNA are then incorporated into the RNA Induced Silencing Complex (RISC) in the cytoplasm of the cell. The RISC consists of Argonaute (Ago) protein as one of its main components. Ago cleaves and discards the passenger (sense) strand of the siRNA duplex giving rise to an active RISC. The remaining (antisense) strand of the siRNA duplex serves as the guide strand and guides the RISC to its homologous mRNA, resulting in the endonucleolytic cleavage of the target mRNA. In human plasma the half-life of the naked siRNA is <1h and is removed through the kidneys even before reaching the target tissues (Rudzinski and Aminabhavi, 2010). In order to improve the stability of siRNA in the blood stream, the siRNA must be bound to a transfection vector or carrier that may be either viral or non-viral. We used this strategy to reduce the expression of beta-catenin in cancer cells.

1.4 Delivery Vehicles

1.4.1 Viral Vectors

A few examples of the most common viral vectors used are retro-virus, herpes simplex virus, lentivirus and adeno-associated viruses each with its therapeutic characteristic (Oligino et al., 2000). The benefit of using viral vectors is their natural ability to enter the cells and express their own proteins. This type of vector allows a high transfection rate and a rapid transcription of the foreign material in the infected host. However the use of viral vectors is limited due to the following concerns. First, gene therapy using viral vectors is limited as only small sequences of DNA can be inserted into the virus genome, making large-scale production of these vectors difficult. Second,

these viruses pose a variety of potential problems such as toxicity, immune responses and inflammatory responses (Sania Mansouri et al., 2004). Lastly oncogenic effects and high costs limit the use of viral vectors. As all these limitations pose i, investigation and development of non-viral vector has been considered.

1.4.2 Cationic Lipids

Cationic Lipids have been routinely used as transfection vectors in tissue culture (Sania Mansouri et al., 2004). The chemistry between these lipids and the negatively charged DNA results in the formation of clusters of aggregated vesicles along the nucleic acid (J.J Wheeler et al., 1999). A variety of cationic lipids have been developed to interact with DNA, but perhaps the best known are N-1(-(2,3-dioleoyloxy)propyl)-N,N,N-trimethylammoniumethyl sulfate (DOTAP) and N-(1-(2,3-dioleoyloxy)propyl)-N,N,N-trimethylammonium chloride (DOTMA). Complexes formed between the cationic lipid and DNA are rapidly cleared from the bloodstream and have been found to be widely distributed in the body (Liu et al., 2002). The transfection efficiency of liposome/DNA complexes in vivo has been shown to be relatively low (Fillion, M.C. Philips., N.C., 1998). These cationic lipids have also been documented to be cytotoxic in nature (Brown et al., 2001). Intravenous injection of stable nucleic acid-lipid particles has successfully targeted the liver to silence the apolipoprotein B (ApoB) gene in mice and nonhuman primates. However, a significant 20-fold transient elevation in serum transaminases (aspartate transaminase, alanine transaminase) indicative of hepatocellular necrosis was identified at the effective dose. Liposomal formulations of nucleic acids are known inducers of inflammatory cytokines including tumor necrosis factor-alpha, interferon-gamma, and interleukin-6 which may be related to liver damage (Alameh et

al., 2012). These disadvantages and variable performance characteristics make cationic lipids unfavorable for use as transfection vectors.

1.4.3 Polyethylenimine

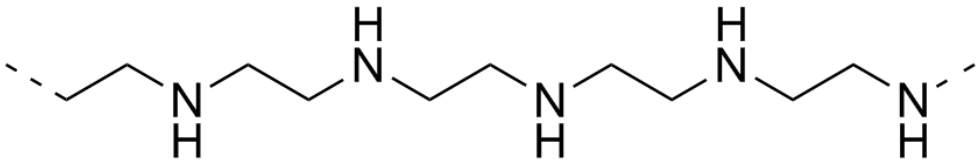

Figure 3: Structure of a linear polyethylenimine

Polyethylenimine (PEI) is a cationic polymer and has been used to facilitate siRNA delivery (Jere et al 2009a, b). Cationic polymers interact with anionic nucleotides to form polyplexes which in turn interact with the cell membrane to promote endosomal uptake and delivery. The polycationic nature of the polymer is responsible for buffering the low endosomal pH through enhanced influx of protons and water resulting in the endosomal rupture and intracellular delivery of polymer and siRNA (Akhtar, S and Benter, I; 2007). It has been reported that at high molecular weight PEI are toxic in nature (Akhtar, S and Benter, I; 2007). The cytotoxic nature of PEI has been defined as a two phase process where the polycation-cell interaction induces loss of cell membrane integrity and the induction of programmed cell death (Alameh et al., 2012). In a study conducted by Pathak et al., (2009) it was reported that PEI exhibits charge associated toxicity which limits its *in vivo* utilization. They were successful however in partially masking the positive charge on PEI through ionic interactions with alginic and hyaluronic acid thus enhancing the cell viability of PEI. In both cases more than 90 % cell viability was scored as compared to 65 % in PEI. Because of toxicity and variable performance, PEI has more constraints for use as a delivery tool for siRNA or oligonucleotides.

1.5 Chitosan as a Transfection Vector

Chitosan (CS) is a naturally occurring polysaccharide composed of glucosamine and N-acetylglucosamine residues derived from partial deacetylation of chitin (generally obtained from Crustacean shells) as shown in Figure 4.

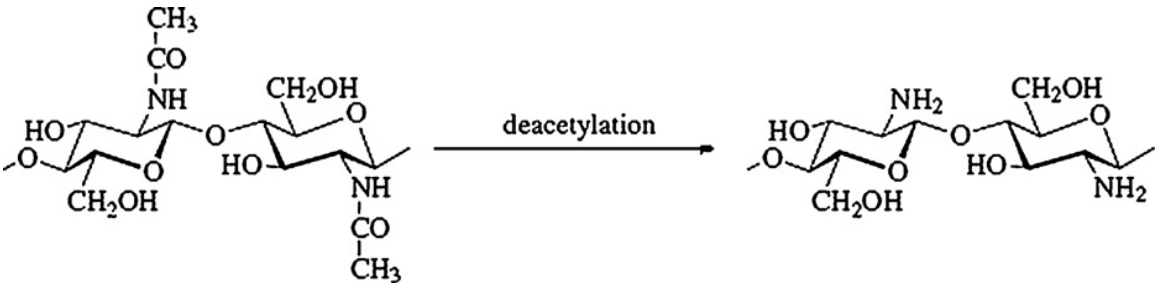

Figure 4: Scheme representing the deacetylation of Chitin. From (Rudzinski et al., 2010)

The amine groups confer a weak basicity to chitosan such that chitosan is soluble in aqueous dilute acids such as hydrochloric or acetic acid when the degree of deacetylation is about 50%. Highly deacetylated chitosans (>85%) are soluble up to a pH of 6.5. Chitosans are normally insoluble under alkaline conditions. Ultimately the solubility is related not only to the degree of deacetylation and pH, but also to the distribution of the acetyl groups along the chain, the ionic concentration, molecular weight and the nature of the acid used for protonation (Leher et al., 1992; He et al., 1998; Casettari et al., 2012). With a p*K*a of approximately 6.5, chitosan is soluble in acidic solutions owing to the protonation of the amino groups composing the polymeric chain at this pH. Chitosan can interact with negatively charged epithelial surfaces or with mucosal surfaces (through an electrostatic interaction with charged sugar groups such as sialic acid) and therefore has been exploited as a bioadhesive material (Casettari et al., 2012). It is now generally accepted that the mechanism of chitosan transport across mucosal

membranes is a combination of bioadhesion (delayed clearance from the site of absorption) and the transient opening of the tight junctions between the epithelial cells of the mucosal membrane (Smith et al.,2004; Illum, L. 2002; Casettari et al., 2012). Chitosan chain length can be decreased by strong acid hydrolysis and biodegraded by a number of enzymes such as lysozyme, di-N-acetylchitobiase, N-acetyl-beta-D-glucosaminidase and chitiotriosidase which are present in human mucosa and other physiological fluids (Illum, L. 1998; Casettari et al., 2012; Garcia-Fuentes et al., 2012).Chitosan has minimal toxicity with half maximal inhibitory concentration (IC_{50}) ranging from 0.2 to 2 mg/ml in most cell lines depending on chitosan's molecular weight and degree of deacetylation (Garcia-Fuentes et al., 2012). Chitosan has low immunogenicity (Muzzarelli et al., 2005). Because of all of these favorable characteristics, chitosan has been extensively employed as a carrier for drugs and nucleic acids.

The use of chitosan as a delivery vector both *in vitro* and *in vivo* for pDNA/siRNA can be traced back to early research conducted by Leong's group (Leong et al., 1998) and more recently reviewed by Garcia Fuentes (Garcia-Fuentes et al., 2012). The protonated amine groups of chitosan (CS) can neutralize the negatively charged siRNA and ultimately facilitate the transport of siRNA across the cell membrane. Additionally, CS shows buffering capacity that is critical for endosomal escape (Chang et al., 2010). Once CS nanoplexes are prepared and inside the cell, they are surrounded by the endosomal membrane and because of the difference in pH inside the cell; the chitosan becomes more protonated. This leads to diffusion of water into the endosome with a concurrent increase in osmotic pressure. Ion influx to counter the positive charge of

chitosan drives the osmotic intake of water into the endosome (hydrogen sponge effect), eventually leading to the disruption of the endocytic membrane and causing a release of the siRNA. Research conducted on multiple cell cultures has proven that CS/pDNA complexes can yield high transfection levels. Strand et al., (2008) have reported that CS/pDNA nanocarriers were successful in achieving positive transfection in about 30-50% of the treated HEK293 cells. The transfection levels in other cell lines such as MCDK, HeLa and Calu-3 were also found to be reduced (Fuente et al., 2008; Teijeiro et al., 2009). Earlier studies have shown that CS/siRNA nanocomplexes are capable of reducing the gene expression by about 50% in HEK 293 cells and human colorectal cancer Lovo cells and these results are similar to the suppression values obtained using Lipofectamine (Lee et al., 2009; Ji et al., 2009; Garcia-Fuentes et al., 2012). We have chosen to develop chitosan nanocarriers for transfection into HCT-116 colon cancer cells in spite of the difficulty in order to make a significant contribution to cancer therapeutics.

1.6 Polyethylene Glycol

In order to make chitosan more soluble in the blood stream we plan to graft copolymerize our chitosan through chemical modification with another polymer, such as poly (ethylene glycol) (PEG). PEG is a linear, hydrophilic, polyether diol that can be synthesized in various molecular weights (0.3-20,000 kDa) and can be functionalized with different terminal end groups such as amino, carboxyl and sulfhydryl groups (Casettari et al., 2012). To obtain a balance between circulation time (favored by larger PEGs) and interaction and uptake into target cells (probably delayed by larger PEGs) the optimal molecular weight range of PEG for grafting unto chitosan is 2-5 kDa (Casettari et al., 2012). It is highly soluble both in water and organic solvents such as methanol,

dichloromethane and chloroform. The use of PEG for pharmaceutical purposes has been approved by the FDA. Minimal cellular adsorption, non-toxic nature, non-immunogenic and non-antigenic properties favor the use of PEG in injectable formulations (Casettari et al., 2012). PEG is biocompatible but is not as biodegradable as poly (lactic-co-glycolic acid) (PLGA), thus necessitating complete toxicological studies to avoid chronic complications. The chemical modification of polymers by PEG improves the pharmacokinetic and pharmacodynamics properties such as increased resistance to immune response in the body, increased hydrophilicity, reduced renal chitosan increases the circulation time of particles in the blood because it is very hydrophilic but not charged. Despite the fact that it is not charged (its zeta potential or surface charge is zero) and thereby does not provide charge repulsion between particles, does provide a hydrophilic appendage around the particle that sterically stabilizes each particle and prevents the aggregation of the particles (Prego et al., 2006). Being hydrophilic, it prevents absorption of blood proteins (opsonins) onto the surface of the particles. The absorption of the proteins leads to rapid recognition by the immune system. Thus, PEG prevents or delays recognition by the immune system. Normally, unmodified polymer particles are rapidly taken up by the macrophages of the liver and spleen which is the way that the body rids itself of these foreign agents. Chitosan can be PEGylated through the carboxyl group of PEG and thus improves its performance. PEG allows CS to retain its inherent characteristics such as molecular structure. The PEG reaction with chitosan nanoplexes is as shown in Figure 5.

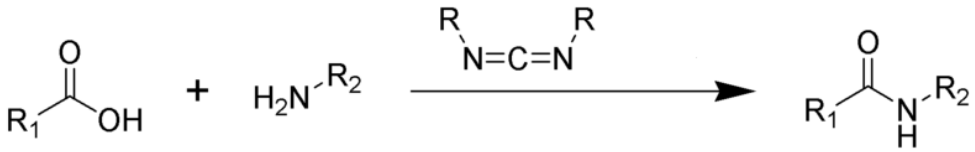

R1 = PEG; R2 = chitosan

Figure 5. Scheme representing formation of the amide linkage using carbodiimide

1.7 Chitosan Nanoplexes in Cancer Therapeutics

As stated earlier, the excellent biocompatibility, complete biodegradability and low toxicity properties of chitosan favor its application in cancer therapy. Lee et al., (2009) have used chitosan-conjugated docetaxel as an oral administration drug. The paper describes how the use of chitosan improves the oral absorption of drug and the residence time of the drug in the blood resulting in increased antitumor efficacy.

Kato et al., (2005) prepared an N-Succinyl-chitosan (Suc-Chi), a chitosan derivative modified by succinyl groups and conjugated it with mitomycin C (MMC) [MMC is a major drug which is used as an anticancer drug conjugated with Suc-Chi in animal studies]. In their paper they reported that chitosan is a good polymeric carrier of anticancer agents. They further reported that Suc-Chi exhibits a remarkable antitumor activity in various tumor models including solid tumors, leukemia and metastatic liver cancer. In another paper by Xu et al., (2009) it was reported that chitosan nanoparticles showed significant dose and size dependent antitumor activity against Sarcoma-180 and hepatoma H22in mice. They further concluded that the chitosan nanoparticles can be considered as a novel class of drug for the treatment of hepatocellular carcinoma (HCC).

1.8 Research Strategy

Chitosan and PEGylated chitosan are being evaluated for their potential to act as delivery vehicles for siRNA. The nanoparticles were prepared and their size and morphology was determined using SEM, TEM and Dynamic light Scattering. ^{1}H NMR analysis of the PEGylated chitosan was used to confirm the degree of deacetylation and determine the percentage PEGylation. The encapsulation efficiency of siRNA was evaluated using UV spectroscopy by determining the amount of free siRNA that would be left out in the supernatant post nanoparticle formation. HCT 116 colorectal cancer cell line was transfected with chitosan/siRNA and PEGylated chitosan/siRNA nanoparticles. The transfection efficiency of the chitosan/siRNA and PEGylated chitosan/siRNA nanoparticles was compared with that of Lipofectamine 2000. Finally the extent of reduction of total cellular beta-catenin was evaluated using western blots. Our ultimate research goal was to synthesize chitosan/siRNA and PEGylated chitosan/siRNA nanoparticles, transfect them into colon cancer cells, and then analyze the extent of beta-catenin protein down regulation.

CHAPTER II

MATERIALS AND METHODS

2.1 Materials

Low molecular weight chitosan (20-300 cP, 1 wt. % in 1 % acetic acid), sodium triphosphate pentabasic (TPP) (M.W 367.86) and silver nitrate were purchased from Sigma-Aldrich (St. Louis, MO, USA). Glacial acetic acid, N-hydroxysuccinimide (NHS) and RNAse free water were obtained from Fisher Scientific (Fair Lawn, NJ, USA). Sodium hydroxide was purchased from EM Science (Gibbstown, NJ, USA). Methoxy poly (ethylene glycol) succinimidyl valerate (mPEG-SVA) (M.W 5000) was purchased from Layson Bio. (Arab, AL, USA). (1-ethyl-3-(3dimethyl amino propyl) carbodiimide (EDC) was obtained from Thermoscientific Pierce (Rockford, IL, USA). NMR tubes were purchased from New Era (Vineland, NJ, USA). Deuterium oxide (99.95% D) and phosphate buffered saline (PBS) were purchased from VWR (San Dimas, CA, USA). Lipofectamine 2000, beta-catenin specific (s436) silencer siRNA (M.W 13300) consisting of sequences where the sense strand is 5′-GGACCUAUACUUACGAAAATT-3′ and the antisensense strand is 5′-UUUUCGUAAGUAUAGGUCCTC-3′ and silencer select negative control, (CTNNB1) RNA (scrRNA) (M.W 13400) were obtained from Life Technologies (Carlsbad, CA, USA). 0.45µm 25mm nylon syringe filters were purchased from Pall Life Sciences (San Diego, CA, USA), 0.22µm 25 mm nylon syringe filters were purchased from Alfa Aesar (Taylor, MI, USA). Snakeskin dialysis tubing (16nm, 10000MWCO) was obtained from Pierce Biotechnology (Rockdale, IL, USA).

Fetal bovine serum (FBS) was purchased from Atlas Biologicals (Ft Collins, CO,USA), monoclonal anti-beta-catenin (catalog #610157) primary antibody from Transduction Laboratories (Beckton Dickinson, CA, USA), monoclonal anti-beta-actin primary antibody produced in mouse clone AC-15 (catalog #A2066) from Sigma Aldrich (St. Louis, MO,USA), secondary antibody from (Santa Cruz Life Sciences, CA, USA), Dulbecco's modified eagle medium (DMEM) from Fisher Scientific (Fair Lawn, NJ, USA), Horseradish Peroxidase Super Signal West Pico Chemiluminescent Substrate kit from Pierce (Rockford, IL, USA). Formvar coated nickel transmission electron microscope grids were purchased from Sigma-Aldrich (St. Louis, MO, USA). HCT-116 cell line was purchased from American Type Culture Collection (Manassas, VA, USA), Pen/strep (1000 U/ml of penicillin and 1000 µg/ml of streptomycin) was purchased from life technologies (Grand island, NY, USA), TEMED (Tetramethylenediamine), 1x PAkt Lysis buffer (20mM Tris pH 7.5, 150mM NaCl, 1mM EDTA, 1mM EGTA, 1% NP-40 and 1% Sodium deoxycholate, 2.5mM Sodium pyrophosphate, 1mM beta-glycerophosphate, 1 mM Sodium Orthovanadate [SO], 1 µg/ml Leupeptin) were generously donated by Dr. Michelle Lane (Texas State University-San Marcos, School of Family and Consumer Sciences).

2.2 MALDI-TOF Characterization of mPEG-SVA

The matrix solution was prepared by dissolving 20 mg of 2,5 dihydroxybenzoic acid (DHB) in one ml of 2:1 acetonitrile/water with 0.1% trifluoroacetic acid (TFA). The sample solution was prepared by dissolving one µl of mPEG-SVA in one ml of the matrix solution. From the matrix solution, three aliquots: 10, 25 and 50 µl were pipetted into three separate Eppendorf tubes. Into each of the Eppendorf tubes, one µl of the

sample solution was pipetted and the mixture vortexed for one min. Two µl of sample was withdrawn from each tube and spotted onto a separate well on a clean stainless steel MALDI target plate. For the control, two µl of matrix solution was spotted onto a separate well of the target plate. The target plate was covered and the spots were dried for one hour. When the spots had dried, the target plate was loaded into the Bruker Autoflex TOF/TOF. A spectrum of mPEG-SVA was obtained in reflector mode between 2-10kDa.

2.3 Synthesis of Poly (ethylene glycol) Grafted Chitosan

Methoxy poly (ethylene glycol) succinimidyl valerate (mPEG-SVA) was grafted onto chitosan using a carbodiimide-mediated reaction as previously described (Ravina et al., 2010). Briefly 100 mg of chitosan (approximately 0.6 µmol) was dissolved in 20 ml of 1% acetic acid solution. The solution was stirred for 20 min and sonicated for about 5 min to get a uniform clear solution. The pH of the solution was then adjusted to 6.3 (the maximum pH in order to maintain solubility) by addition of 1.0 M NaOH solution. 17.8 milligram (3.09 µmol) of mPEG-SVA and 2.02 mg (0.017 mmol) of NHS were then added to the solution. Finally 27.3 mg (0.142 mmol) of EDC (a zero length cross-linking agent that initiates the reaction between carboxyl group of PEG and the amine groups of chitosan to yield an amide linkage) was added to the solution. The solution was stirred at room temperature for 22 hours. The resulting solution was then filtered using 10000 MWCO micro-separation dialysis tubing. A portion (about one ml) of the solution was lyophilized producing 105 mg of white foam, and then analyzed using ^{1}H NMR.

2.4 NMR Characterization of Poly (ethylene glycol) Grafted Chitosan

The ^{1}H NMR spectrum of the copolymer was obtained in D_2O using a Bruker 400 MHz NMR spectrometer. The samples were prepared by dissolving 1 mg of the sample in 1 ml of D_2O. The degree of PEGylation was determined by comparing the methoxy peak at 3.42 of mPEG with the peak at 2.06-2.10 from chitosan.

2.5 Preparation of Chitosan-siRNA Nanoparticles

Nanoparticles were prepared using an ionotropic gelation technique according to the methodology previously described (Bertthold et al., 1996). Briefly 100 mg of chitosan was dissolved in 20 ml of 1% acetic acid solution. The solution was stirred for 20 min and then sonicated for about 5 min to get a uniform clear solution. The pH of the solution was then adjusted to 6.3 by addition of 1.0 M NaOH solution. The chitosan solution containing about 24 ml was then filtered twice; first using a 0.45 µm nylon syringe filter followed by a second filtration using a 0.22 µm filter in order to remove aggregates. 280 µl of sodium triphosphate pentabasic (TPP) at a concentration of 2.5 mg/ml (0.57 µmol P) was mixed with 120 µl of 40 µM siRNA (4.8 nmol; 0.20 µmol P). For the negative control 280 µl of TPP at a concentration of (2.5 mg/ml; 0.57 µmol P) was mixed with 120 µl of 40 µM scrRNA (4.8 nmol; 0.20 µmol P). 30 µl of either TPP/siRNA or TPP/scrRNA solution was then added to one ml of chitosan solution and then vortexed for 5 sec. The process was repeated until all of the TPP/siRNA or TPP/scrRNA was added to the chitosan solution. The nanoparticles formed spontaneously. Based on the molecular weight as obtained from a MALDI-TOF experiment (166,000 Da) and using the weighted average molecular weight of the glucosamine and acetylated glucosamine monomer units, the average number of N were calculated. Given 0.47 µmol of N in the

chitosan, the N/P ratio is 0.61. The nanoparticles were then placed in the refrigerator at 4 °C for one hour so that the nanoparticles would precipitate, after which they were then centrifuged at 13467 *x* g (G-force) for 120 minutes at 4 °C using an Allegra X-22 R centrifuge (Beckman Coulter). The supernatants after centrifugation were saved for evaluation of loading efficiency. The pelleted nanoparticles were then treated with 1ml of RNAse-free water and then vortexed vigorously to evenly suspend the nanoparticles.

2.6 Preparation of Chitosan-Silver Nanocomposite

Chitosan-Silver nanocomposite was prepared using a protocol previously described (Murugadoss et al., 2007). A beaker containing 50 ml of Milli-Q water was placed in an oil bath maintained at a temperature range of 93-95 °C. 100 mg of chitosan was added into the beaker. One ml of 20 mM silver nitrate solution was added to the chitosan, which was followed by addition of 100 µl of 0.3 M NaOH solution. The resultant solution turned yellow in a minute indicating the formation of chitosan-silver nanocomposite. The reaction was allowed to continue for an additional 10 minutes. The beaker was then taken out from the oil bath and cooled to room temperature. The pH of the solution was found to be 9.4. The powdered yellow colored solid was separated and washed five times with Milli-Q water. The solid was air dried and was now ready for further use. About 40 mg of silver attached chitosan was dissolved in 20 ml of 0.1 % (v/v) acetic acid. The pH of the solution was about 4.3. NaOH solution was added drop-wise in order to adjust the pH of the solution to 6.3. About 8 ml of 0.4 mg/ml solution of sodium triphosphate pentabasic (TPP) was then added to the solution. This immediately resulted in the formation of chitosan-silver nanoparticles.

2.7 Preparation of PEGylated Chitosan/siRNA Nanoparticles

Nanoparticles were prepared using an ionotropic gelation technique according to the methodology previously described (Bertthold et al., 1996). The PEGylated chitosan solution was filtered twice; first using a 0.45 µm nylon syringe filter followed by a second filtration using a 0.22 µm filter in order to remove aggregates. For the positive control 280 µl of sodium triphosphate pentabasic (TPP) at a concentration of 2.5 mg/ml (0.57 µmol P) was mixed with 60 µl of 40 µM siRNA (2.4 nmol ; 0.10 µmol P). For the negative control 280 µl of TPP at a concentration of 2.5 mg/ml (0.57 µmol P) was mixed with 60 µl of 40 µM scrRNA (2.4 nmol; 0.10 µmol P). 30 µl of either TPP/siRNA or TPP/scrRNA solution was then added to one ml of PEGylated-chitosan solution and then vortexed for 5 sec. The process was repeated until all of the TPP/siRNA or TPP/scrRNA was added to the PEGylated chitosan solution. The nanoparticles formed spontaneously. Given 0.47 µmol of N in the chitosan, the N/P ratio is 0.70. The nanoparticles were then placed in the refrigerator at 4 $^{\circ}$C for an hour after which they were then centrifuged at 13467 x g (G-force) for 120 minutes at 4 $^{\circ}$C. The supernatants were saved for evaluation of loading efficiency. The pelleted nanoparticles were then treated with 1ml of RNAse free water and then vortexed vigorously to evenly suspend the nanoparticles. In the initial experimental trials that were conducted 0.1 nmol of siRNA was encapsulated in the PEGylated chitosan. For this purpose 30 µl of 40 µM siRNA (1.2 nmol; 0.050 µmol P) was mixed with 280 µl of sodium triphosphate pentabasic (TPP) at a concentration of 2.5 mg/ml (0.57 µmol P). Similarly for the negative control; 30 µl of 40 µM scrRNA (1.2 nmol; 0.050 µmol P) was mixed with 280 µl of sodium triphosphate pentabasic (TPP) at a concentration of 2.5 mg/ml (0.57 µmol P). The subsequent steps were the same as

mentioned earlier. Given 0.47 µmol of N in the chitosan, the N/P ratio is 0.75. In an attempt to achieve maximum encapsulation efficiency we also mixed 120 µl of siRNA (0.20 µmol P) with 280 µl of TPP (0.57 µmol P) and 120 µl of scrRNA (0.20 µmol P) with 280 µl of TPP (0.57 µmol P), then proceeded to prepare the nanoparticles as previously described. Given 0.47 µmol of N in the chitosan, the N/P ratio was 0.61.

2.8 Estimation of siRNA Encapsulation Efficiency

Serial dilutions of both siRNA and scrRNA at different known concentrations were made and tested for absorbance at a wavelength of 260 nm using a NanoDrop (Thermo Scientific, Wilmington, DE, USA). The absorbance of the supernatant from the PEGylated chitosan without any siRNA/scrRNA was used as a blank. The volume of sample used to detect the absorbance was 1 µl. The absorbance of the supernatant from PEGylated chitosan nanoparticles encapsulated with either siRNA or scrRNA were then measured. A standard curve was obtained by plotting absorbance against the amount of RNA present. The amount of RNA in the supernatant was then determined using the equation from the slope of the standard curve. The amount of RNA in the supernatant was subtracted from the total amount of RNA added to the nanoparticles; the difference was then divided by the total amount of RNA added to the nanoparticles and multiplied by 100 to be represented as a percentage. This percentage represents the amount of RNA encapsulated in the PEGylated chitosan nanoparticles. The same procedure was used to evaluate the percentage encapsulation in chitosan nanoparticles.

2.9 Characterization of the nanoparticles

2.9.1 Scanning Electron Microscopy (SEM)

The size and morphology of nanoparticles were analysed using the Helios NanoLab 400 DualBeam scanning electron microscope from FEI Co. (Hillsboro, OR, USA). For SEM analysis, 1 µl of each sample was placed on a small piece of aluminum tape and allowed to dry overnight. The size and morphology of the nanoparticles were observed, measured and imaged in secondary mode (low energy electrons [< 50 eV] that are ejected from the atoms in the sample by inelastic interactions with beam electrons) and backscatter electron (BSE) mode (consists of high-energy electrons originating in the electron beam, that are reflected or back-scattered out by elastic scattering interaction with specimen atoms) under vacuum.

2.9.2 Transmission Electron Microscopy (TEM)

The size and morphology of nanoparticles were analysed using a transmission electron microscope (TEM) JEM 1200 EXII from JOEL Ltd. (Tokyo, Japan). For TEM analysis 1 µl of chitosan-silver nanocomposite was added to 100 µl of RNase free water. Each TEM sample was then plated onto a nickel TEM grid and then stained with 2 % phosphotungstic acid for 2.20 minutes. The grids were then taken off the stain and allowed to air dry. Size and morphology were then observed with the TEM under vacuum conditions.

2.9.3 Zeta Potential and Size Measurement

The mean particle size and the size distribution of the nanoparticles were determined using dynamic light scattering (DLS). The zeta potential values of the nanoparticles were found by Laser Doppler Anemometry (LDA), measuring the average

electrophoretic mobility. Samples of nanoparticle suspensions were diluted with 10mM KCl. The DLS and the LDA analyses were performed with a Zetasizer Nano ZS (Malvern Instruments, Germany).

2.10 Culture of HCT 116 Colon Cancer Cells

To test whether our chitosan/RNA and PEGylated chitosan/RNA nanoparticles are effective in reducing the beta-catenin protein level, the human colon cancer cell line HCT-116 was cultured as recommended by the American Type Culture Collection (Manassas, VA). Specifically HCT-116 cells were cultured in Dulbecco's modified eagle medium (DMEM) media, supplemented with 10% FBS and antibiotics (1000 U/ml of penicillin and 1000 μg/ml of streptomycin). To determine the transfection efficiency the cells were plated in a six-well plate at a density of 2.12×10^5 cells per well in DMEM media supplemented with 10 % FBS. Each experiment was repeated three times.

2.11 Transfection of Colon Cancer Cells with Lipofectamine

To examine if siRNA transfected using Lipofectamine could reduce beta-catenin protein levels, HCT-116 cells were treated with Lipofectamine (200 pmol/μl) containing either 0.1 nmol or 0.5 nmol of siRNA (positive control) or 0.5 nmol of scrRNA (negative control). The treatment of HCT-116 cells with scrRNA was used as a reference to normalize the reduction in beta-catenin protein levels. Twenty four hours after treatment, the transfection media was replaced with 1 ml of DMEM (lacking FBS and antibiotics). The RNA treatment was then evaluated at both the 24 h and 48 h time points. A stock solution of phosphate buffer saline/sodium orthovanadate (PBS/SO) was prepared by mixing (200 μl of 200 mM SO in 40 ml PBS). SO is an inhibitor of protein tyrosine phosphatases and inhibits the

phosphorylation of a protein of interest by inhibiting endogenous phosphatases present in a cell lysate mixture. To harvest the protein from the cells, the media was poured out and the cells were treated with one ml of a mixture of PBS/SO solution. The cells were scraped and transferred to an Eppendorf tube. The Eppendorf tubes were then centrifuged at 3387 rcf at 4 °C for 5 min. While the cells were spinning 5 µl of Phenylmethylsulfonyl fluoride (PMSF [is a serine protease inhibitor]) was added to 500 µl of PhosphoAkt (PAkt) lysis buffer. The supernatant in the Eppendorf tubes was then discarded and 60 µl of (PMSF-PAkt) lysis buffer was added to the pellets. The Eppendorf tubes were vortexed to dissolve the cells in the lysis buffer. The solution was sonicated for about 10 seconds and the tubes were incubated in ice for 20 min. The Eppendorf tubes were then centrifuged at 18440 rcf at 4 °C for 10 min. The supernatants were transferred to fresh Eppendorf tubes and stored in ice.

2.12 Transfection of Colon Cancer Cells with Chitosan/siRNA

To examine if siRNA transfected using chitosan could reduce beta-catenin protein levels, HCT-116 cells were treated with chitosan/siRNA nanoparticles. HCT-116 cells were also treated with chitosan/scrRNA where the scrRNA was not expected to reduce any cellular beta-catenin protein levels. Before treatment chitosan/siRNA and chitosan/scrRNA nanoparticles were concentrated by centrifugation at 7889 *x* g for 10 min. The resulting pellet was dissolved in DMEM and the resulting solution was the transfection medium. The transfection medium was then passed through a sterile 0.2 µm syringe filter. One ml of transfection media was then added to each well. Each well received 500 pmol of RNA (either siRNA or scrRNA). Twenty-four hours after treatment the transfection medium was replaced with 1 ml of DMEM (lacking FBS and antibiotics).

Cells were harvested 24 h and 48 h later. A stock solution of PBS/SO (Sodium orthovanadate) was prepared by mixing (200 µl of 200 mM SO in 40 ml PBS). To harvest the protein from cells the media was poured out and the cells were washed with one ml of a mixture of PBS/SO solution. The cells were scraped and transferred to an Eppendorf tube. The Eppendorf tubes were centrifuged at 3387 rcf at 4 °C for 5 min. While the cells were spinning 5 µl of phenylmethylsulfonyl fluoride (PMSF) was added to 500 µl of PhosphoAkt (PAkt) lysis buffer. The supernatant in the Eppendorf tube containing the cells was discarded and 60 µl of (PMSF-PAkt) lysis buffer was then added to the pellets. The Eppendorf tubes were vortexed to dissolve the cells in the lysis buffer. The solution was sonicated for about 10 seconds and the tubes were incubated in ice for 20 min. The Eppendorf tubes were then centrifuged at 18440 rcf at 4 °C for 10 min. The supernatants were transferred to fresh Eppendorf tubes and stored in ice.

2.13 Transfection of Colon Cancer Cells with PEGylated Chitosan/siRNA

To examine if siRNA transfected using PEGylated chitosan could reduce beta-catenin protein levels, HCT-116 cells were treated with PEGylated chitosan/siRNA nanoparticles. HCT-116 cells were also treated with PEGylated chitosan/scrRNA, where the scrRNA was not expected to reduce any cellular beta-catenin protein levels. Before treatment PEGylated chitosan/siRNA and PEGylated chitosan/scrRNA nanoparticles were concentrated at 7889 *x* g for 10 minutes. The resulting pellet was dissolved in DMEM and the resulting solution was the transfection medium. The transfection medium was then passed through a sterile 0.2 µm syringe filter. One ml of transfection media was then added to each well. Each well received 500 pmol of RNA (either siRNA or scrRNA). 24 h after treatment the transfection media was replaced with one ml of

DMEM (lacking FBS and antibiotics). To harvest the protein from cells the medium was poured out and the cells were washed with one ml of a mixture of PBS/SO solution. The cells were scraped and transferred to an Eppendorf tube. The Eppendorf tubes were then centrifuged at 3387 rcf at 4 °C for 5 min. While the cells were spinning 5 µl of Phenylmethylsulfonyl fluoride (PMSF) was added to 500 µl of PhosphoAkt (PAkt) lysis buffer. The supernatant was discarded and 60 µl of (PMSF-PAkt) lysis buffer was added to the pellets. The Eppendorf tubes were then vortexed to dissolve the cells in the lysis buffer. The solution was sonicated for about 10 seconds and the tubes were incubated in ice for 20 min. The Eppendorf tubes were then centrifuged at 18440 rcf at 4 °C for 10 min. The supernatant was transferred to fresh Eppendorf tubes and stored in ice.

2.14 Western Immunoblot Analysis

Western immunoblot analysis for beta-catenin was performed as described in (Dillard et al. 2007). An aliquot of 5 µl of protein harvested from the cells was quantified in a spectrometer using the BioRad DC protein assay kit (Hercules, CA, USA). One hundred µg of protein per lane was electrophoresed through a 10% SDS-PAGE gel and then transferred to a nitrocellulose membrane. Membranes were blocked with 5% milk in Tris buffered saline and Tween-20 (TBST) (10 mM Tris, pH 8, 150 mM NaCl, and 0.5% Tween-20) for 1 h at room temperature. After the first blocking step beta-catenin antibody (Beckton Dickinson, catalog #610157, CA,USA) and beta-actin antibody (added as a control for protein) (Sigma Aldrich catalog #A2066, St. Louis, MO, USA) were added at 1:1000 dilution and 1:5000 dilutions, respectively. The membrane was incubated with 5% milk in TBST and primary antibodies for one hour at room temperature. After incubation with the primary antibodies the membrane was washed 1x

with TBST for five minutes. The membrane was incubated with 5% milk with secondary antibody (1:10000 dilutions) for 60 min. After incubation with the corresponding secondary antibody, the membrane was washed 3x with TBST for five minutes each time. Immunoreactivity was detected with the Pierce Horseradish Peroxidase Super Signal West Pico Chemiluminescent Substrate kit and the western blot image was obtained using FOTODYNE system (Hartland, WI, USA). The image was quantified using ImageQuant TL 7.0 image analysis software (GE Healthcare Biosciences, Uppsala, Sweden).

CHAPTER III

RESULTS

3.1 MALDI-TOF Analysis

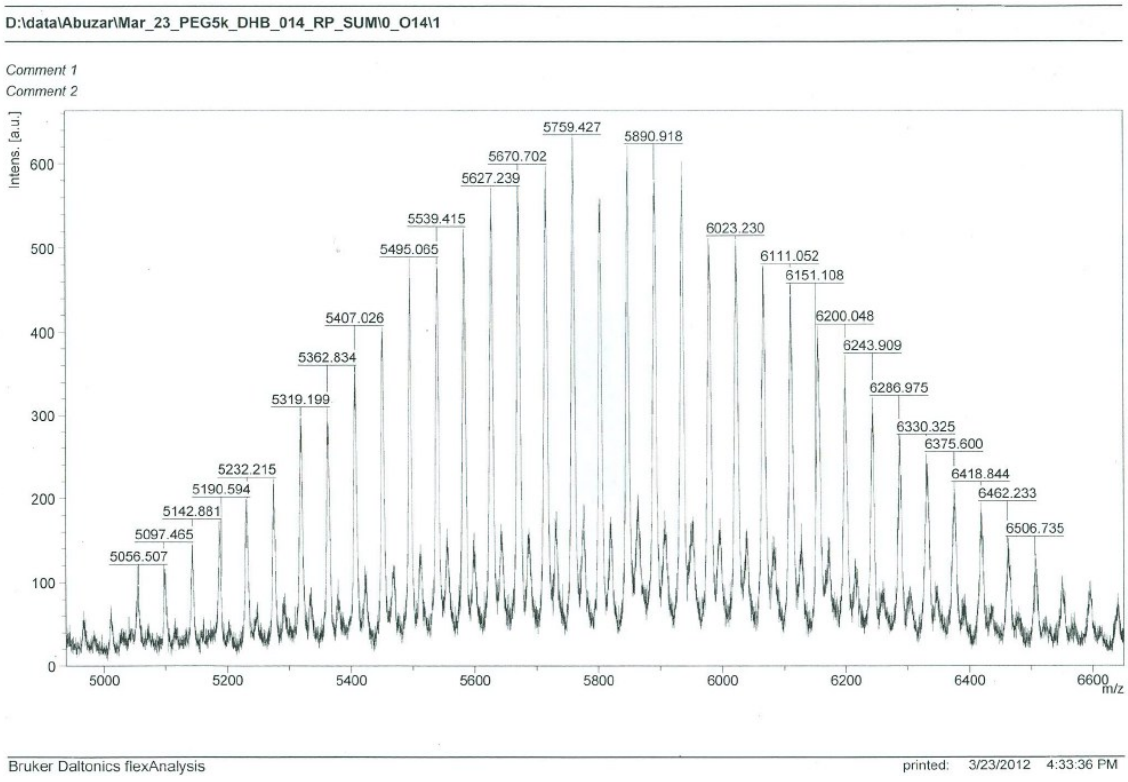

Figure 6. MALDI TOF analysis of mPEG-SVA

Figure 6 is the MALDI-TOF spectrum for mPEG-SVA. The MALDI-TOF analysis of mPEG-SVA valerate yielded a number average molecular weight Mn of 5,759 (estimate) which was calculated using the following equation $Mn = \sum_i NiMi/\sum_i Ni$, and corresponded with 124 ethyl ether monomer units. The weight average molecular weight Mw of 6200 (estimate) was calculated using the following equation $Mw = \sum_i NiMi^2/\sum_i NiMi$. A polydispersity index (PDI) of 1.07 was obtained by using Mw/Mn.

3.2 NMR Analysis Data

3.2.1 ^{1}H NMR of Chitosan

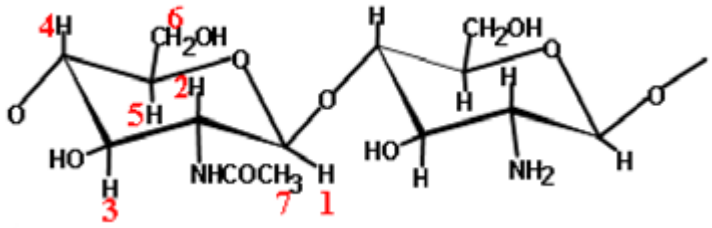

Figure 7: Chitosan structure From (Young et al., 2008) [Copyright Elsevier Publishers, 2008).

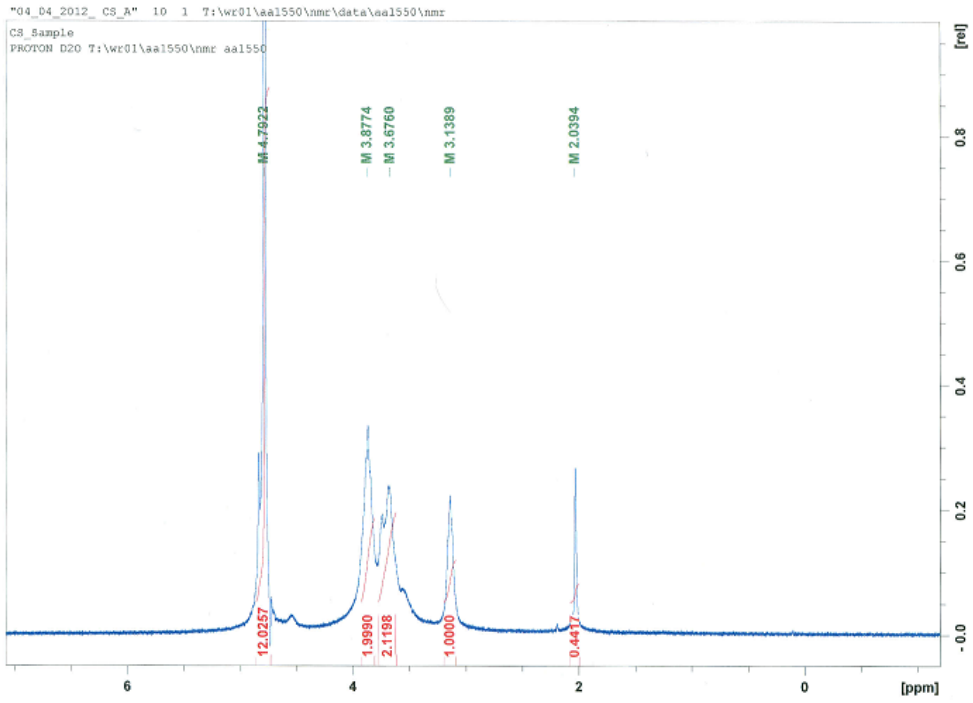

Figure 8: ^{1}H NMR of Chitosan (D_2O, TMS)

Figure 7 depicts the structure and numerical designation for all of the protons in Chitosan while Figure 8 is the H^1 NMR of chitosan. The Chitosan H^1 NMR depicts chemical shifts at δ 2.03 (HAc, 3 acetyl protons of acetyl glucosamine), δ 3.14 (proton 2

of acetylglucosamine as well as the corresponding proton in glucosamine), δ 3.68, δ 3.74 and δ 3.86 (undefined signals attributed to chitosan). (Young et al., 2007) δ 4.79 comes from HOD in the D_2O solvent. Using the following formula, the degree of deacetylation can be determined (ASTM F2260) (Lavertu et al., 2003)

$$DD = i_{3.14}/(i_{3.14} + i_{2.04}/3) \qquad (1)$$

Where DD is the degree of deacetylation, $i_{3.14}$ is the integrated intensity at 3.14 ppm and correlated with the proton attached to the carbon next to the amine/amide group of chitosan and $i_{2.04}$ is the integrated intensity at 2.04 ppm and correlated with the three protons of the acetyl group of acetylglucosamine. Based on an integrated intensity of 1.00 for the peak at 3.14 and an integrated intensity of 0.441 for the peak at 2.04 ppm, the degree of deacetylation (DD) is 87% for the low molecular weight chitosan. Integration values are present on the spectrum for reference purposes, and each number represents the approximate number of hydrogen's that the peak is associated with, in the compound.

3.2.2 H^1 NMR of mPEG-SVA

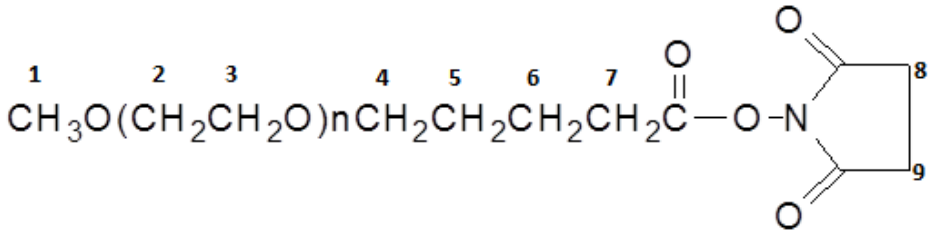

Figure 9: Structure of Methoxy poly (ethylene glycol) succinimide (mPEG-SVA)

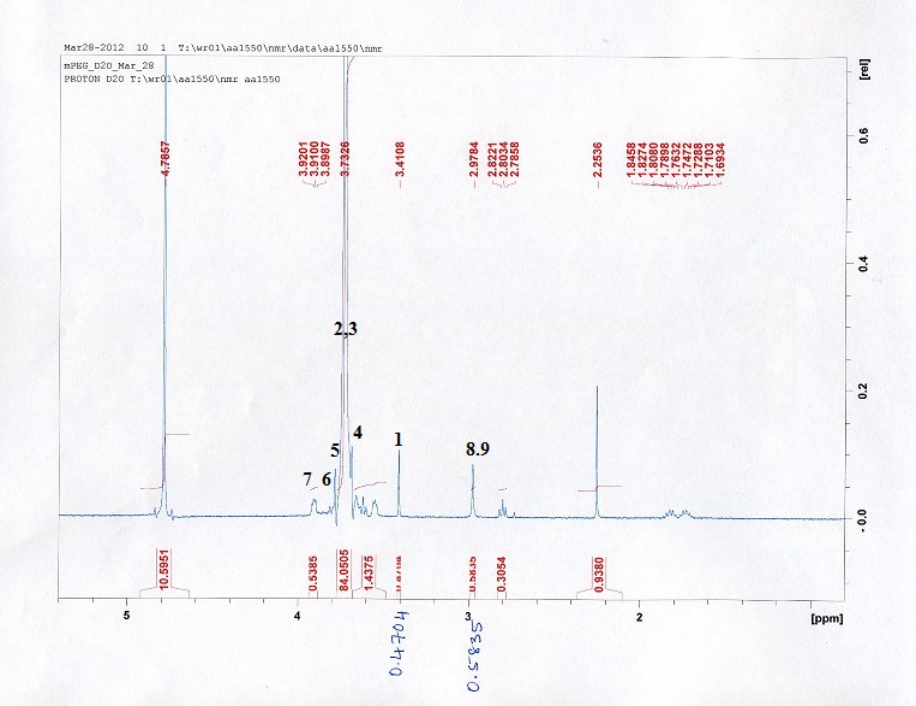

Figure 10: ^{1}H NMR of mPEG-SVA (D_2O, TMS):

Figure 9 depicts the structure and numerical designation for all of the protons in mPEG-SVA while Figure 10 is the H^1 NMR of mPEG-SVA. The mPEG-SVA H^1 NMR depicts chemical shifts at δ 1.69-1.84 multiplet (weak) and is unassigned, δ 2.25 is a singlet (sharp) and unassigned, δ 2.78-2.82 is a triplet (weak) and is unassigned, δ2.97 is a singlet (medium) and has been assigned to the methylene protons adjacent to the imide, δ 3.41 is a singlet (sharp) and has been assigned to the methoxy group terminating the PEG, δ 3.73 is an intense signal (broad) and is assigned to the polyether protons of the PEG, δ 3.89-3.92 is a triplet (weak) and assigned to the methylene protons adjacent to the carboxyl group, δ 4.79 comes from HOD in the D_2O solvent (Young et al., 2007).

The number of ethyl ether units in the PEG chain can be determined by comparing the peak intensity at 3.73 ppm with that at 3.41 ppm using the following formula:

$$EE\ units = (i_{3.73}/4)/(i_{3.41}/3)$$

Where an EE unit represents the number of ethyl ether units in PEG, $i_{3.73}$ is the integrated intensity at 3.73 ppm and correlated with the ethyl ether protons of PEG and $i_{3.41}$ is the integrated intensity at 3.41 ppm and correlated with the terminal methoxy group of mPEG. Based on an integrated intensity of 159.56 for the peak at 3.73 ppm and an integrated intensity of 1.009 for the peak at 3.41 ppm, the number of ethyl ether monomer units is 120 yielding a molecular weight of 5,250 for mPEG-SVA (assuming that none of the succinimide has hydrolyzed). The number of ethyl ether monomer units is very close to the value obtained from a MALDI-TOF analysis which yielded a number average molecular weight of 5,759 (estimate) and 124 ethyl ether monomer units, Integration values are present on the spectrum for reference purposes and each number represents the approximate number of hydrogen's that the peak is associated with, in this compound.

3.2.3 H^1 NMR of 1-ethyl-3-(3dimethyl amino propyl) carbodiimide (EDC)

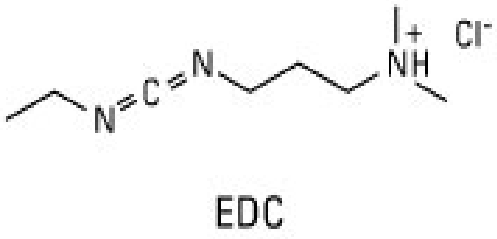

EDC

Figure 11: EDC structure

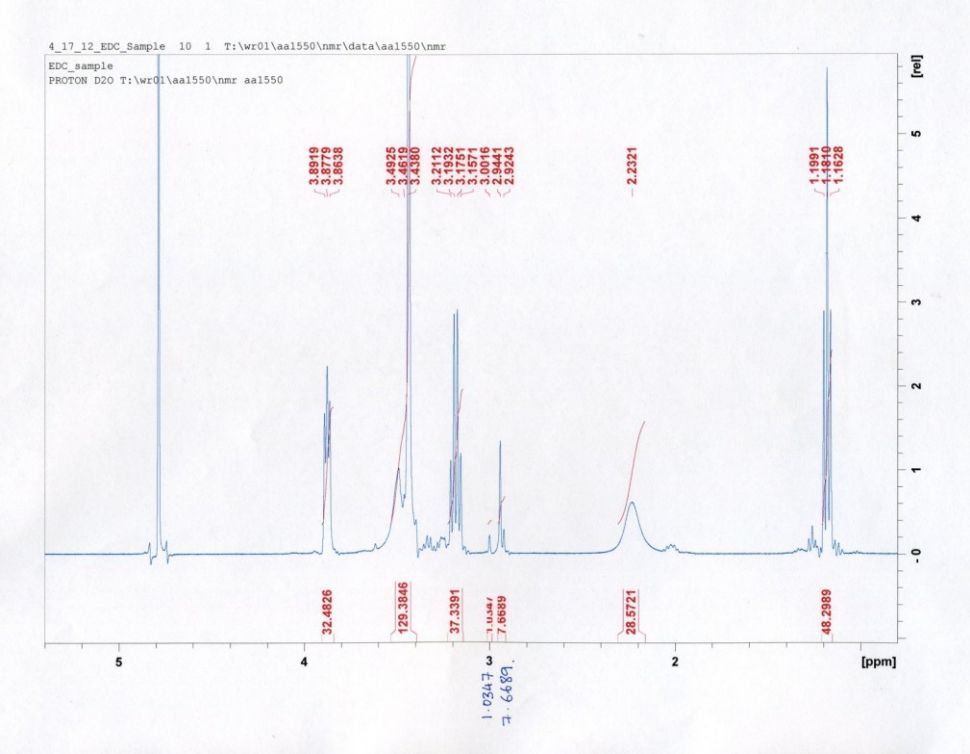

Figure 12: ^{1}H NMR of EDC (D_2O, TMS)

Figure 11 depicts the structure of EDC while Figure 12 is the H^1 NMR of EDC. The H^1 NMR of EDC depicts chemical shifts at δ 1.16-1.19 is a triplet (sharp), δ 2.23 represents a singlet (broad), δ 2.92-3.00 represents a multiplet (medium), δ 3.15-3.21 represents a quartet (sharp), δ 3.43-3.49 represents a multiplet (strong), δ 3.86-3.89 represents a triplet (sharp). δ 4.79 represents the HOD in the D_2O solvent. Integration values are present on the spectrum for reference purposes, and each number represents the approximate number of hydrogen's that the peak is associated with, in this compound.

3.2.4 H^1 NMR of Chitosan-mPEG

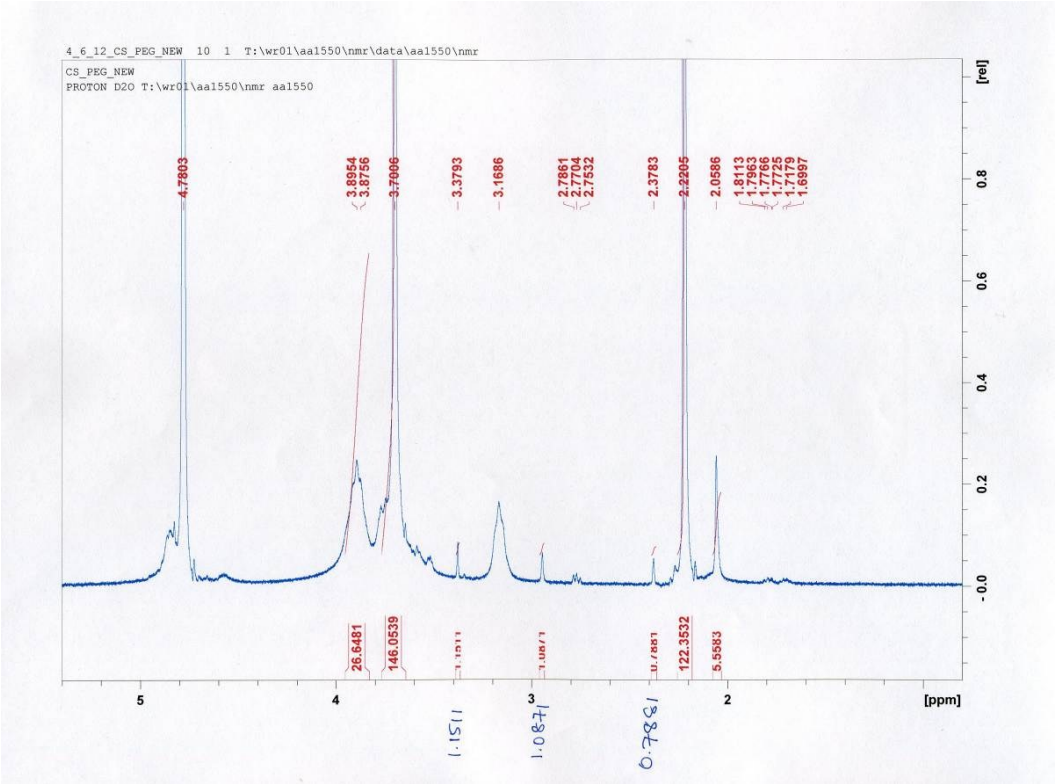

Figure 13: ^{1}H NMR of Chitosan mPEG-SVA mixture (D_2O, TMS):

After mixing the chitosan with mPEG-SVA, H^1 NMR (Figure 13) was obtained in order to determine the chemical shifts associated with each reagent prior to bonding. The Chitosan mPEG-SVA mixture has the following chemical shifts:

δ 1.69-1.81 represents a multiplet (weak) and is associated with mPEG-SVA, δ 2.05 represents a singlet (sharp) corresponding to the 3 acetyl protons of acetyl glucosamine, δ 2.22 a multiplet (broad) is associated with mPEG-SVA, δ 2.37 represents a singlet (weak) and is unassigned, δ 2.97 represents a singlet (weak) corresponding to the methylene protons of mpeg-SVA adjacent to the imide, δ 3.16 represents a singlet (broad) is associated with the chitosan and has been assigned to the proton 2 of

acetylglucosamine as well as the corresponding proton in glucosamine, δ 3.37 represents a singlet (weak) and has been assigned to the methoxy group terminating the PEG, δ 3.70-3.85 represents multiple peaks (broad) corresponding to the polyether protons of the PEG. δ 4.79 represents the HOD in the D_2O solvent. Integration values are present on the spectrum for reference purposes, and each number represents the approximate number of hydrogen's that the peak is associated with, in this compound.

3.2.5 H^1 NMR of PEGylated Chitosan before Filtration

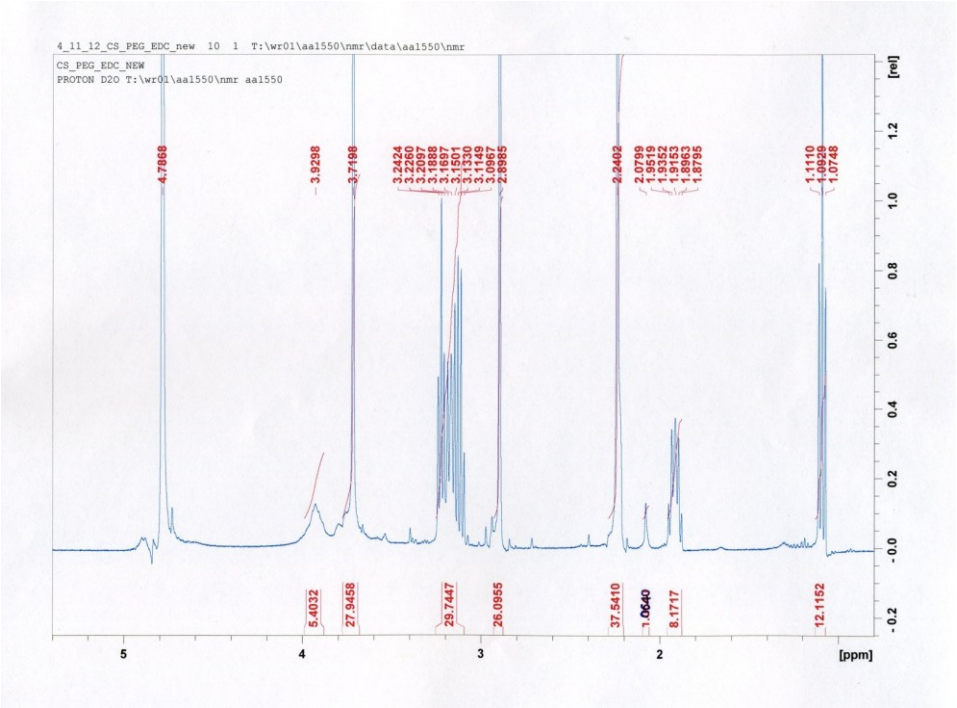

Figure 14: ^{1}H NMR of PEGylated Chitosan unfiltered (D_2O, TMS):

Figure 14 depicts the ^{1}H NMR of PEGylated chitosan before filtering any unreacted mPEG-SVA and EDC and has the following chemical shifts:

δ 1.07-1.11 represents a triplet (strong) and is associated with EDC, δ 1.87-1.95 represents a quintet (medium) and is unassigned, δ 2.07 represents a singlet (weak)

corresponding to the 3 acetyl protons of acetyl glucosamine, δ 2.24 represents a singlet (sharp) and is associated with EDC, δ 2.89 has been assigned to the methylene protons adjacent to the imide in mPEG-SVA, δ 3.09-3.24 represents a multiplet (sharp) and is obscuring a peak associated with chitosan, δ 3.71-3.92 represents a multiplet and is associated with mPEG and chitosan. δ 4.79 represents the HOD in the D_2O solvent. Integration values are present on the spectrum for reference purposes, and each number represents the approximate number of hydrogen's associated with either chitosan, mPEG-SVA,EDC or PEGylated chitosan.

3.2.6 H^1 NMR of PEGylated Chitosan (D_2O, TMS):

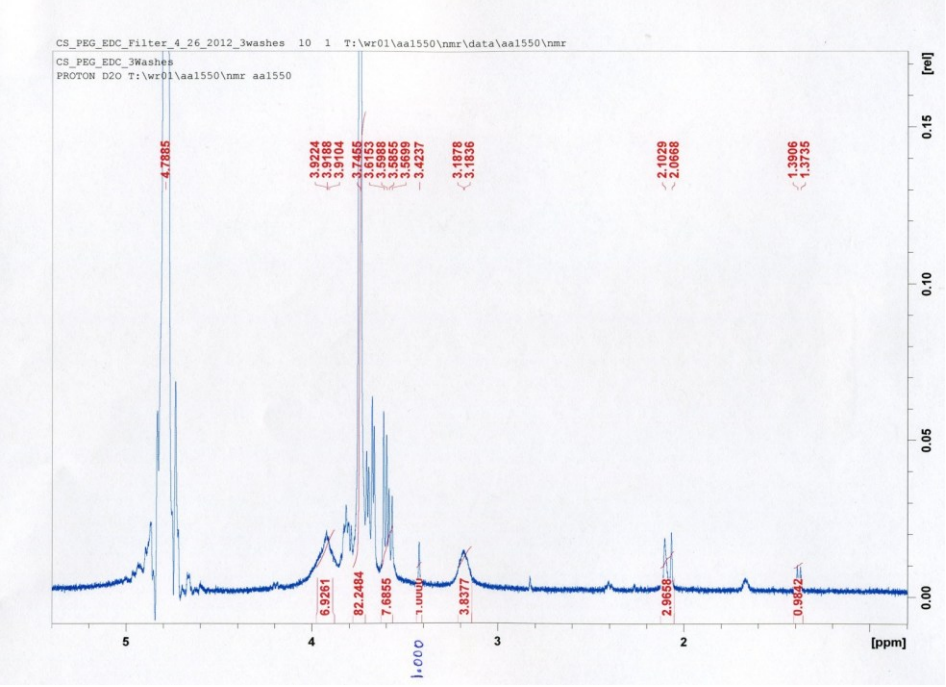

Figure 15: ^1H NMR of PEGylated Chitosan (D_2O, TMS):

Figure 15 depicts the ^1H NMR of PEGylated chitosan after removing any of the unreacted mPEG-SVA and EDC has the following chemical shifts:

δ 1.37-1.39 represents a doublet (weak) and is unassigned, δ 2.06-2.10 represents a doublet (medium) corresponding to the 3 acetyl protons of acetyl glucosamine, δ 3.18

represents a singlet (broad) that is associated with chitosan and has been assigned to proton 2 of acetylglucosamine as well as the corresponding proton in glucosamine, δ3.42 represents a singlet (weak) and has been assigned to the methoxy group terminating the PEG, δ 3.56-3.74 represents a multiplet (sharp) corresponding to the polyether protons of the PEG, δ 3.91-3.92 represents a multiplet (broad) corresponding to the chitosan. δ 4.79 represents the HOD in the D_2O solvent. Integration values are present on the spectrum for reference purposes, and each number represents the approximate number of hydrogen's that the peak is coupled to in the molecules of PEGylated chitosan.

The following equation can be used to determine the number of polyethylene glycol units attached to the chitosan:

$$\text{Number of PEGs} = I_{3.42}/(i_{2.06\text{-}2.10}(1\text{-DD}))$$

Here, $i_{3.42}$ is the integrated intensity at 3.42 ppm and correlates with the three terminal methoxy protons of PEG and $i_{2.07}$ is the integrated intensity between 2.06-2.10 ppm and correlates with the three acetyl protons of acetylglucosamine. Since the number of acetylglucosamine units in the chitosan is only 13% (1-DD), by taking this into account, the number of PEG's attached to the chitosan can be determined. Based on an integrated intensity of 1.000 for the peak at 3.42 ppm and an integrated intensity of 2.97 for the two peaks between 2.06-2.10 ppm, the Number of PEGs is 2.59 per chitosan.

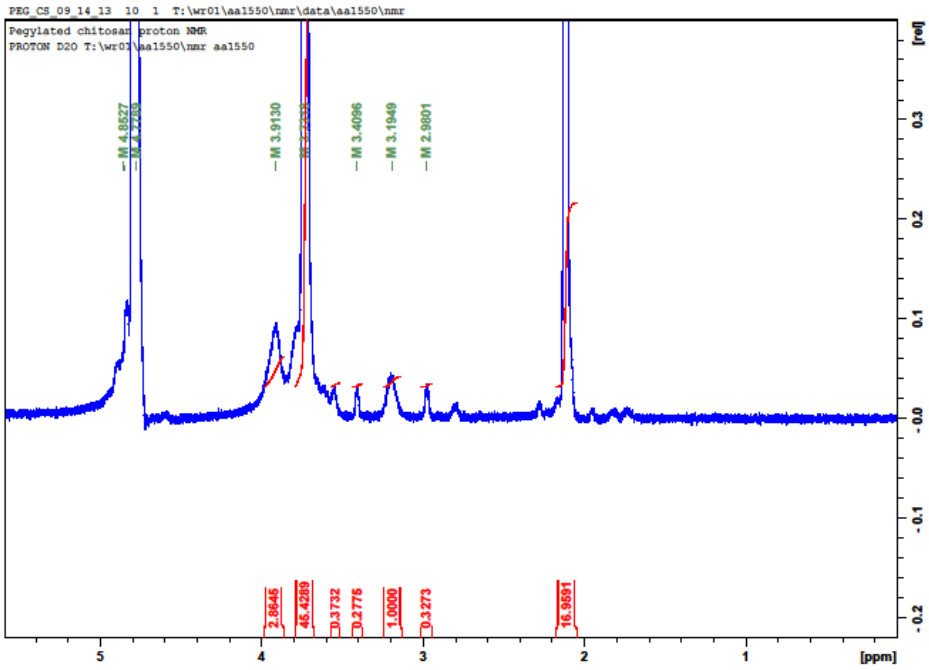

Figure 16: ^{1}H NMR of PEGylated Chitosan (D_2O, TMS):

Figure 16 depicts the^{1}H NMR of PEGylated chitosan which was used as a delivery vector for the treatment of HCT-116 cells. Based on an integrated intensity of 0.2775 for the peak at 3.40 ppm and an integrated intensity of 16.9591 for the peak at 2.10 ppm, the Number of PEGs is .125 per chitosan.

3.3 Estimation of siRNA Encapsulation Efficiency

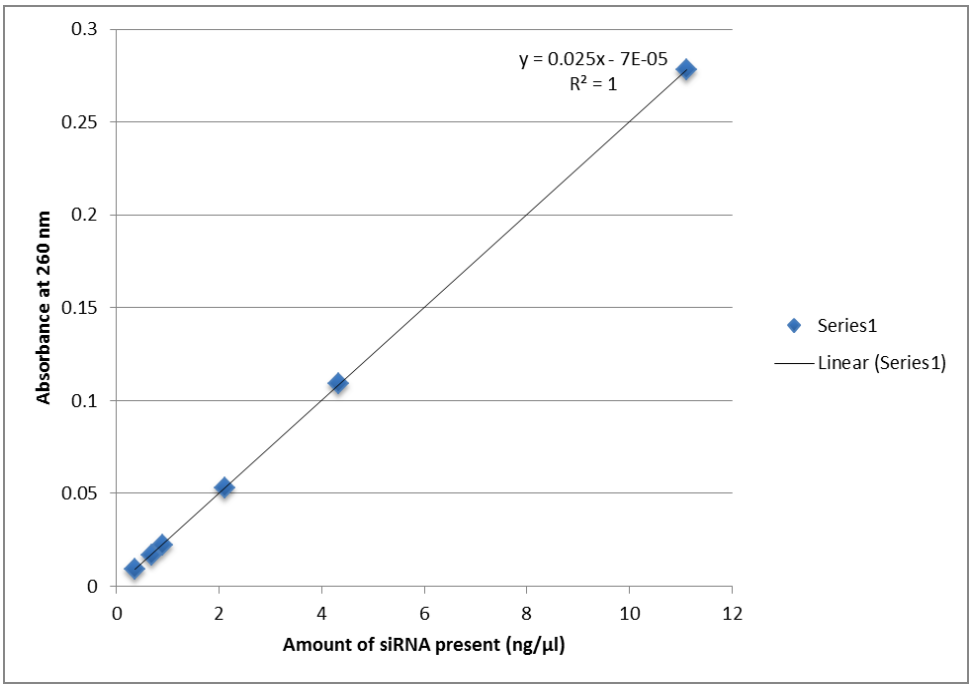

Figure 17: Anti-beta-catenin siRNA serial dilution graph

The encapsulation efficiency of siRNA in the chitosan and PEGylated chitosan nanoparticles (NP's) was determined, in order to estimate the concentration of siRNA that was used to treat the colorectal cancer cells. The absorbance at known concentrations of siRNA was determined and a trend line applied to the graph. The slope of the line in the graph was used to estimate the concentration of non-encapsulated siRNA in the supernatant of chitosan/siRNA and PEGylated chitosan/siRNA preparations. The encapsulation efficiency of anti-beta-catenin siRNA in chitosan/siRNA NP's and PEGylated chitosan/siRNA NP's is as shown in Table 1. When 120 µl of 40 µM siRNA (4.8 nmol) was used the encapsulation efficiency for the PEGylated chitosan/siRNA NP's decreased indicating that we had surpassed the saturation point for encapsulation.

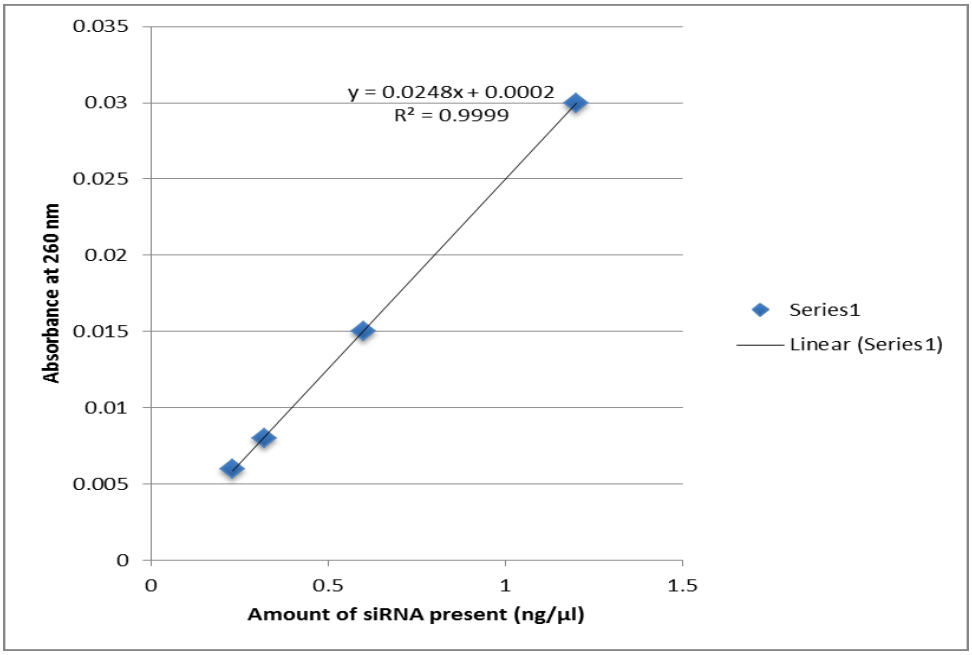

Figure 18: scrRNA serial dilution graph

The encapsulation efficiency of scrRNA in the chitosan and chitosan-PEG NP's was determined in order to estimate the concentration of scrRNA that was added to the colorectal cancer cells. The absorbance at known concentrations of scrRNA was determined and a trend line was applied to the graph. The slope of the line in the graph was used to estimate the concentration of non-encapsulated scrRNA in the supernatant of chitosan/scrRNA and PEGylated chitosan/scrRNA preparations. The encapsulation efficiency of scrRNA in chitosan/scrRNA NP's and PEGylated chitosan/scrRNA NP's is as shown in Table 2. When 120 µl of 40 µM scrRNA (4.8 nmol) was used the encapsulation efficiency decreased indicating that we had surpassed the saturation point for encapsulation.

Table1: Anti-beta-catenin siRNA encapsulation efficiency data

NP Delivery Vector	Amount of siRNA added (nmol)	Amount of siRNA encapsulated (nmol)	Amount of siRNA non-encapsulated (nmol)	% efficiency
Chitosan/siRNA	1.2	0.81	0.39	67.19
Chitosan/siRNA	4.8	3.13	1.67	65.23
PEGylated Chitosan/siRNA	1.2	1.14	0.06	95.26
PEGylated Chitosan/siRNA	2.4	2.58	-0.18	107.65
PEGylated Chitosan/siRNA	4.8	1.12	3.68	23.25

Table2: Non-silencing scrRNA encapsulation efficiency data

NP Delivery Vector	Amount of siRNA added (nmol)	Amount of siRNA encapsulated (nmol)	Amount of siRNA non-encapsulated (nmol)	% efficiency
Chitosan/scrRNA	4.8	3.30	1.50	68.67
PEGylated Chitosan/scrRNA	1.2	1.18	.02	98.55
PEGylated Chitosan/scrRNA	2.4	1.04	1.35	43.61
PEGylated Chitosan/scrRNA	4.8	1.19	3.60	24.94

3.4 SEM Analysis of Chitosan and PEGylated Chitosan Nanoparticles

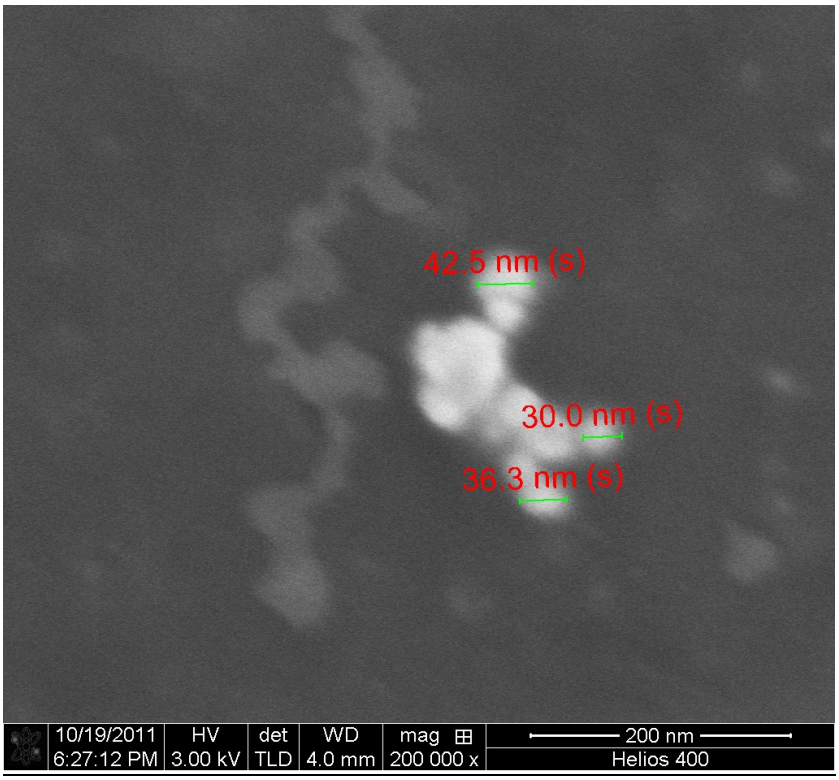

Figure 19: SEM image of Chitosan nanoparticles

Figure 19 is the SEM image of Chitosan nanoparticles without any encapsulated siRNA. The average size of the nanoparticles is between 30 and 43 nm based on a limited though representative estimation of the size of the nanoparticles.

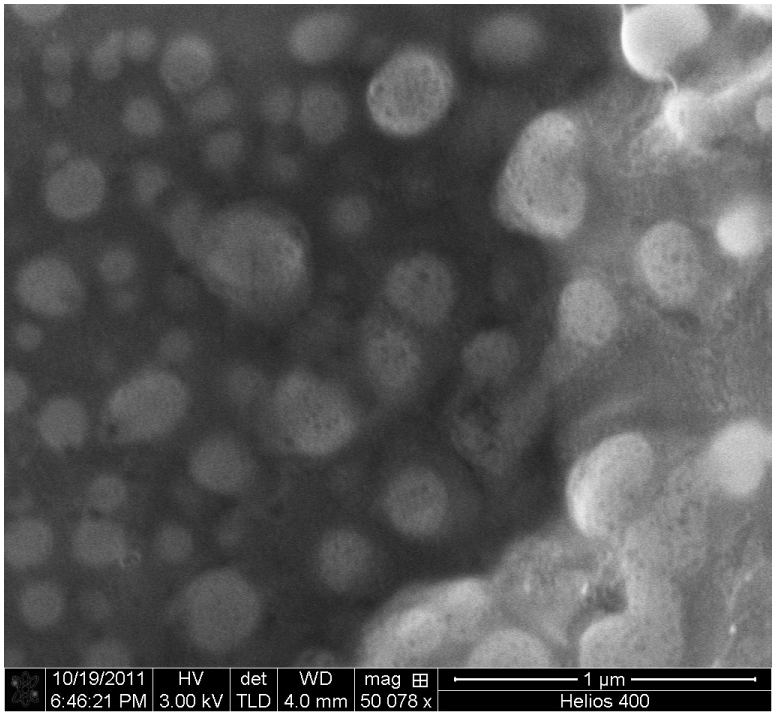

Figure 20: SEM image of Chitosan-silver nanocomposite

Figure 20 is the SEM image of chitosan-silver nanocomposite without any encapsulated siRNA. As seen in the Figure the nanoparticles are spherical in shape. The particles that do not appear to be aggregated (in the background) appear to range from 100-300 nm.

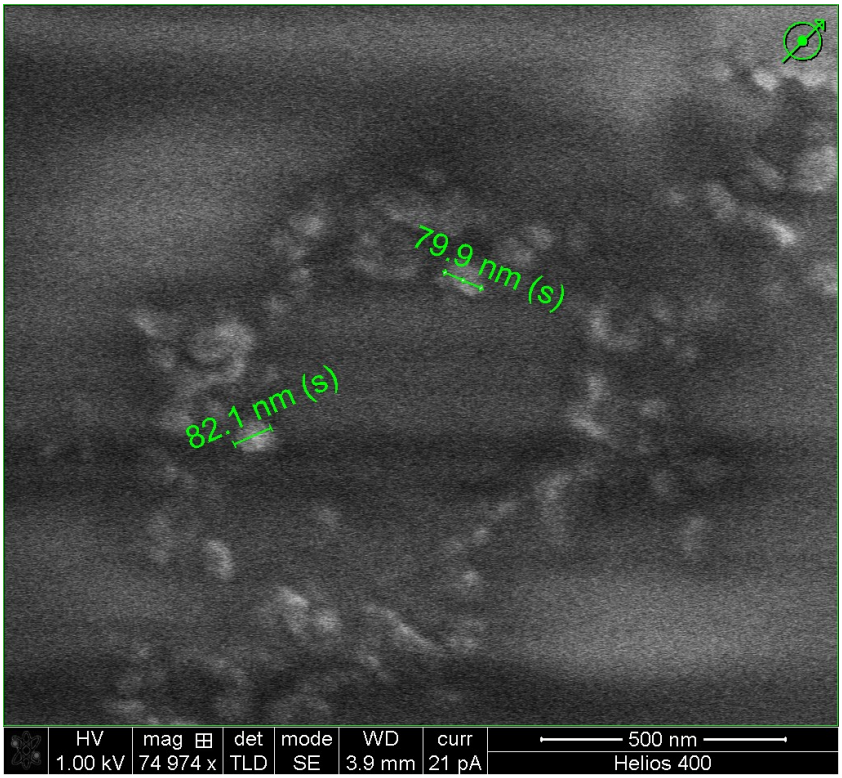

Figure 21: SEM image of PEGylated Chitosan

Figure 21 is the SEM image of PEGylated chitosan nanoparticles without any encapsulated siRNA. The average size of the PEGylated chitosan nanoparticles is about 80 nm.

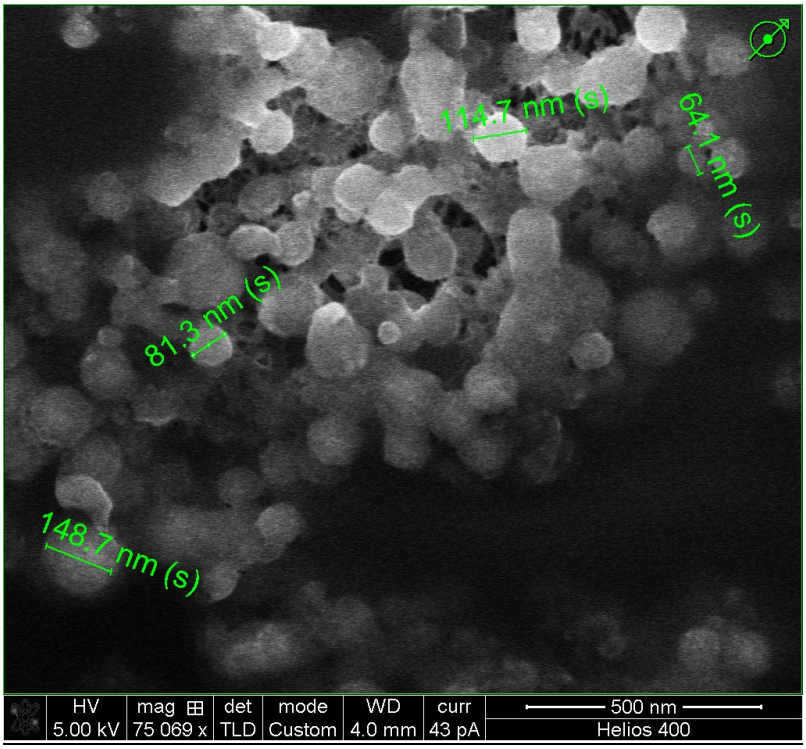

Figure 22: SEM image of PEGylated Chitosan/siRNA

Figure 22 is the SEM image of PEGylated chitosan/siRNA nanoparticles. The average size of the nanoparticles is around 100 nm and is larger on average than the size of PEGylated chitosan nanoparticles without any encapsulated siRNA while also exhibiting a greater polydispersity.

3.5 TEM Analysis of Chitosan-Silver Nanocomposites

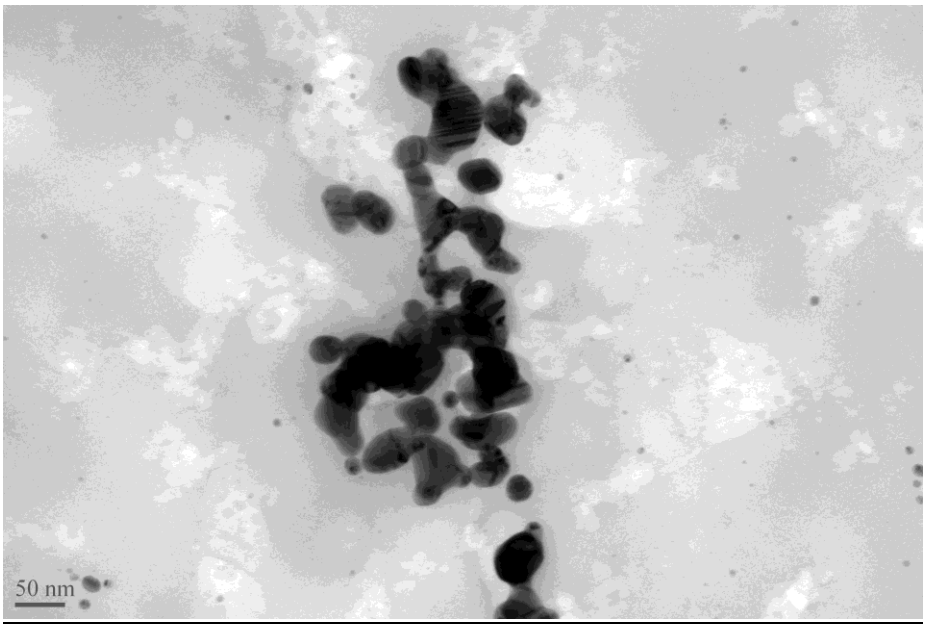

Figure 23: TEM image of Chitosan-silver nanocomposites

Figure 23 shows a TEM image of the chitosan-silver nanocomposites. Silver being an electron dense agent was used solely for the purpose of visualization and trying to obtain an image at greater magnification. The TEM images provided a better evaluation of the morphology of chitosan nanoparticles. There appears to be some aggregation of the nanoparticles, and an average size below 50 nm. Figure 24 is a zoomed-in TEM image of a single chitosan-silver nanocomposite showing a very bulbous and compact structure.

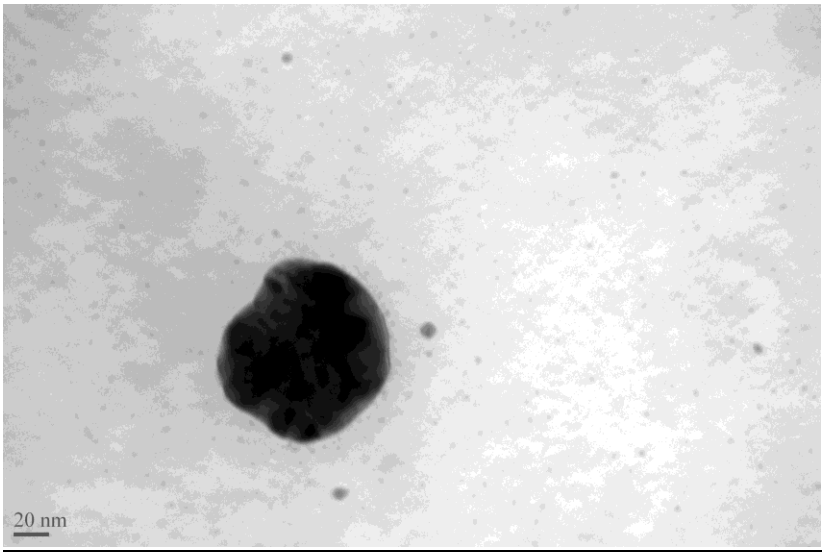

Figure 24: TEM image of Chitosan-silver nanocomposite

3.6 Zeta Potential Data of Chitosan and PEGylated Chitosan Nanoparticles

Temperature (°C):	25.0	Zeta Runs:	12
Count Rate (kcps):	157.4	Measurement Position (mm):	2.00
Cell Description:	Clear disposable zeta cell	Attenuator:	11

		Mean (mV)	Area (%)	Width (mV)
Zeta Potential (mV):	25.6	Peak 1:	25.6	100.0	3.86
Zeta Deviation (mV):	3.86	Peak 2:	0.00	0.0	0.00
Conductivity (mS/cm):	0.774	Peak 3:	0.00	0.0	0.00

Result quality : Good

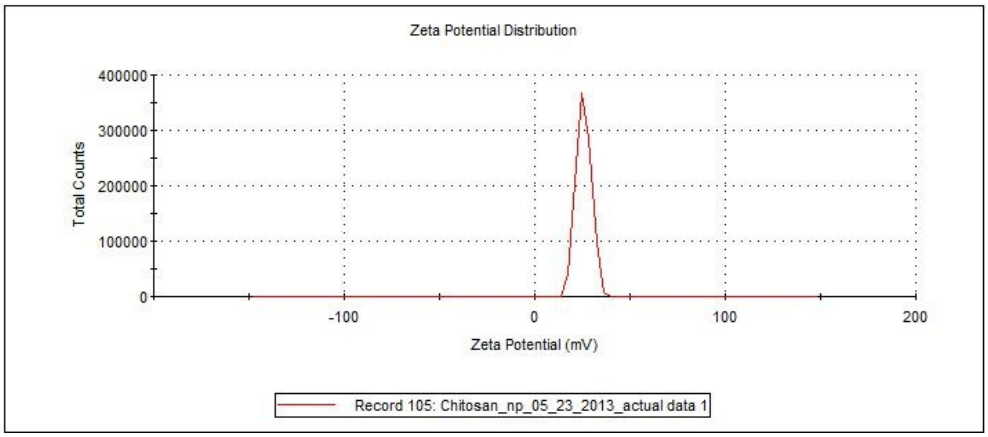

Figure 25: Zeta potential of Chitosan/siRNA (0.1 nmol) nanoparticles

As seen from Figure 25 chitosan nanoparticles have a positive zeta potential of 26 mV. The protonated amine groups of chitosan are responsible for the positive surface charge.

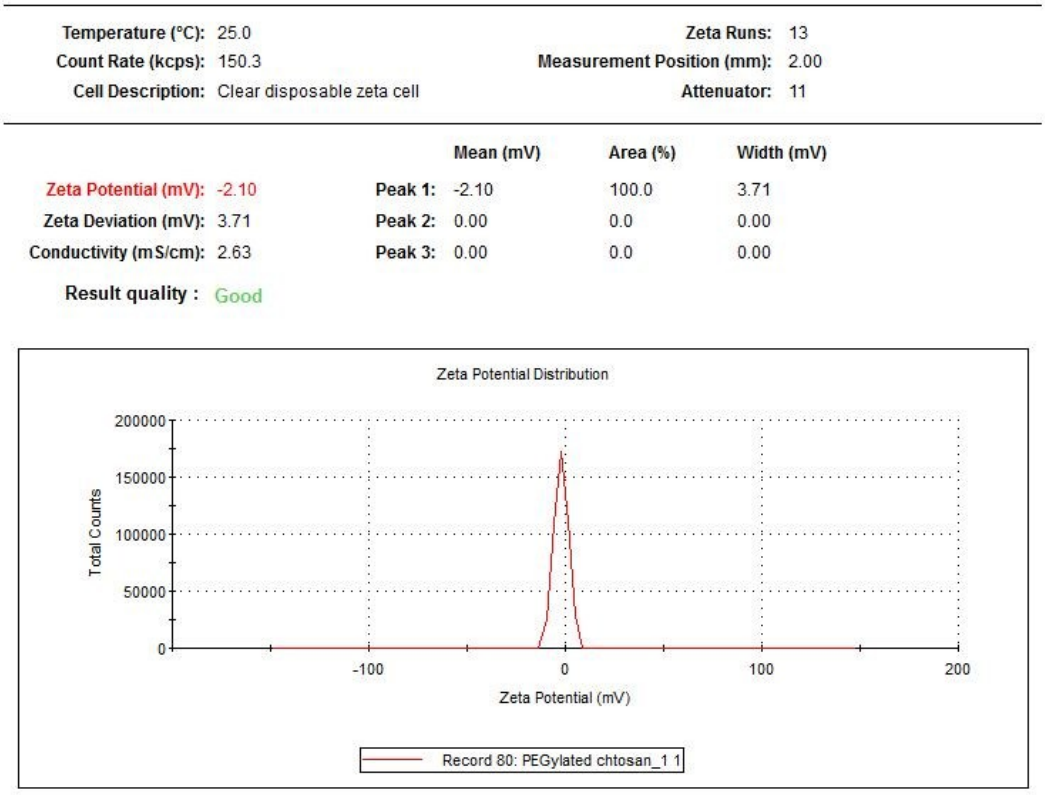

Figure 26. Zeta potential of PEGylated chitosan/siRNA (0.1 nmol) nanoparticles

As seen from Figure 26. PEGylated chitosan/siRNA has an almost zero zeta potential (-2 mV). The attachment of poly (ethylene glycol) reduces the surface charge of chitosan nanoparticles by providing a hydrophilic shell around the nanoparticles making them water-soluble and improving their biocompatibility.

3.7 Evaluation of beta-catenin Reduction in HCT-116 Cells Treated with LF/siRNA

HCT-116 cells

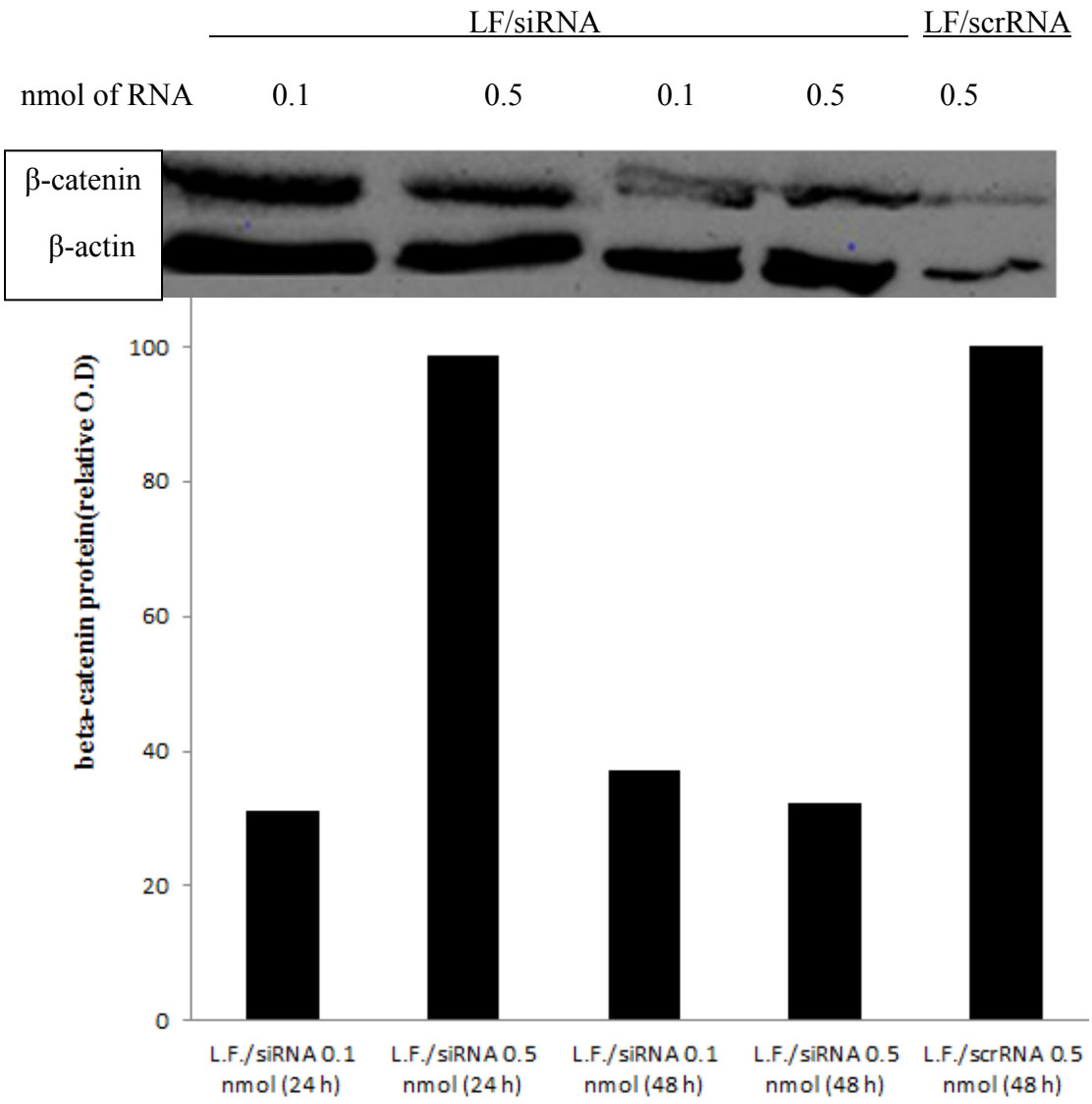

Figure 27. Lipofectamine/siRNA (LF/siRNA) decreases total cellular beta-catenin protein. HCT-116 cells were plated and treated with 0.1 and 0.5 nanomoles of siRNA for 24 h (LANE 1-2) and 48 h (LANE 3-4). Treatment of cells with Lipofectamine/scrRNA (LF/scrRNA) (LANE5) was also included to compare the level of beta-catenin protein between lanes. Following treatment the proteins were harvested, electrophoresed and probed with beta-catenin and beta-actin antibodies as described in section 2.14. This experiment was done only once and thus mean and standard deviation values are not represented.

The HCT-116 cell line exhibited a reduction in total cellular beta-catenin protein in 3 of 4 experiments to approximately 30% of the negative control in response to treatment with 0.1 and 0.5 nmol of anti-beta-catenin siRNA at 24 h and 48 h. Transfection with LF/siRNA (0.5 nmol) for 24 hour was an exception as it did not decrease the cellular beta-catenin protein level. Because the results were promising, we decided to evaluate the reduction of beta-catenin following treatment of the HCT-116 cells with chitosan/siRNA (CS/siRNA) nanoparticles and also with PEGylated chitosan/siRNA (PEG CS/siRNA) nanoparticles.

3.8 Evaluation of beta-catenin Reduction in HCT-116 Cells Treated with 0.1 nmol of RNA

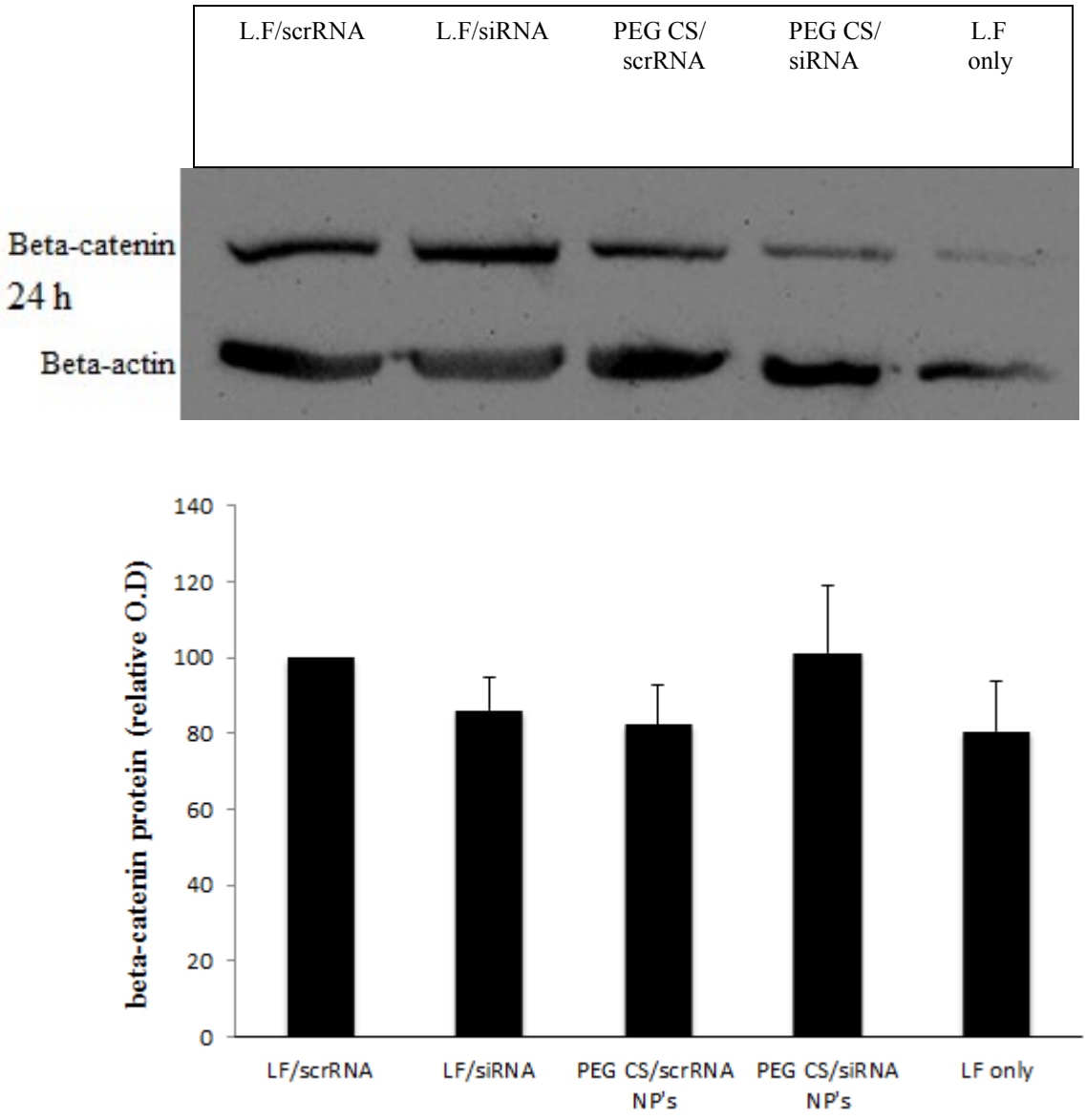

Figure 28. Pegylated chitosan/siRNA(PEG CS/siRNA) did not decrease the total cellular beta-catenin protein level. HCT-116 cells were plated and transfected with 0.1 nanomoles of siRNA and 0.1 nanomoles of scrRNA (in case of negative control) per well for 24 hours. Following treatment the proteins were harvested, electrophoresed and probed with beta-catenin and beta-actin antibodies as described in section 2.14. Beta-actin was used to demonstrate equal loading. The percent reduction in cellular beta-catenin protein was calculated by dividing total beta-catenin by total beta-actin and normalizing to vehicle control treated cells transfected with LF/scrRNA. This experiment was performed three times with similar results; one representative western blot is shown. Values shown are the mean of three separate experiments ± SEM.

LF/siRNA was used as a positive control to compare the reduction in total cellular beta-catenin level when compared to cells treated with PEGylated chitosan/siRNA (PEG CS/siRNA). HCT-116 cells did not decrease the total cellular beta-catenin protein level in response to treatment with 0.1 nmol of siRNA where PEGylated chitosan was the delivery vector. HCT-116 cells which did not receive any siRNA treatment were also included in this experiment to compare the total cellular beta-catenin protein level with those cells that were treated with siRNA. We observed that cells treated with PEG CS/siRNA did not reduce beta-catenin protein levels. Also as seen in Figure 28 the cells which did not receive any siRNA treatment had a lower cellular beta-catenin protein level when compared to those treated with PEG CS/siRNA. This comparison added to our conclusion that the treatment with 0.1 nmol of siRNA encapsulated in PEGylated chitosan nanoparticles did not decrease beta-catenin protein levels in HCT-116 cells when the amount of siRNA is 0.1 nmol. Apparently the amount of beta-catenin expressed in the cells is so high that a larger amount of siRNA needs to be incorporated in order to induce an effect.

3.9 Evaluation of beta-catenin Reduction in HCT-116 Cells Treated with 0.5nmol of RNA

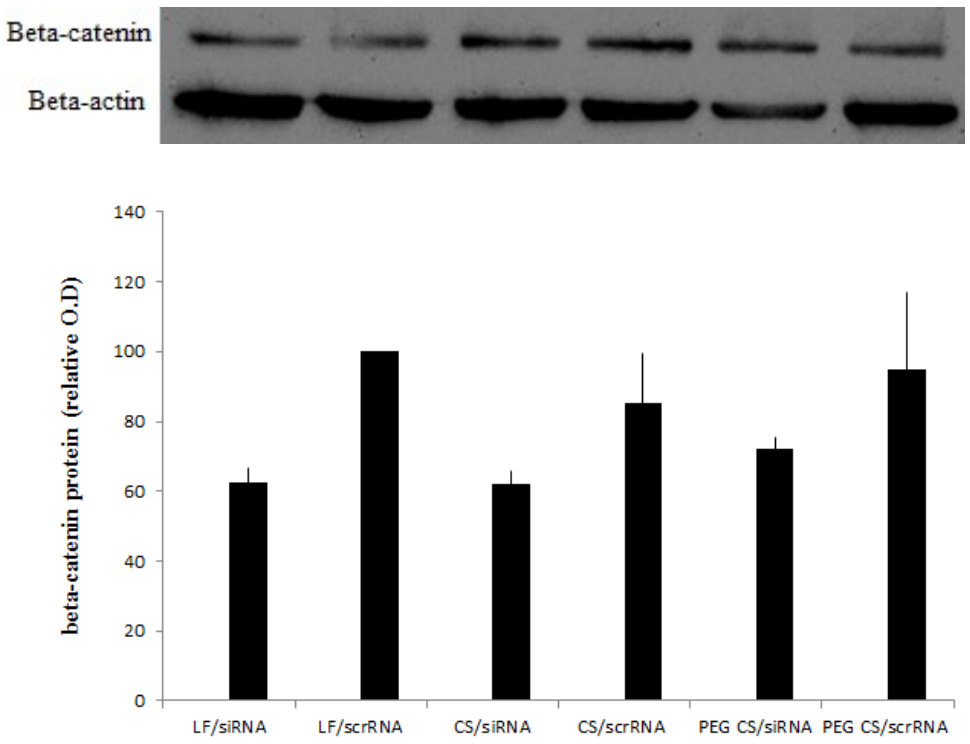

Figure 29. Chitosan/siRNA (CS siRNA) and PEGylated chitosan/siRNA (PEG CS/siRNA) treatments successfully reduced cellular beta-catenin protein level after 24 h. HCT-116 cells were plated and treated with 0.5 nanomoles per well of either siRNA or scrRNA encapsulated in either LF, CS or PEG CS for 24 h. Following treatment the proteins were harvested, electrophoresed and probed with beta-catenin and beta-actin antibodies as described in section 2.14. This experiment was performed three times with similar results; one representative western blot is shown for each time point. Below the western blot for each time point is a histogram with aligned bars that represent the percentage reduction in cellular beta-catenin protein level relative to beta actin for each blot. Values shown are the mean of three separate experiments ± SEM.

Figure 29 shows the results for HCT-116 cells transfected with chitosan/siRNA (CS/siRNA) and PEGylated chitosan/siRNA (PEG CS/siRNA) or a corresponding negative control [chitosan/scrRNA (CS/scrRNA) and PEGylated chitosan/scrRNA (PEG

CS/scrRNA)], after 24h. Lipofectamine/siRNA (LF/siRNA) has been used as a positive control to compare the reduction in total cellular beta-catenin level with those cells treated with PEG CS/siRNA and CS/siRNA. Both CS/siRNA and LF/siRNA treated cells exhibited a reduction in total cellular beta-catenin protein levels to approximately (62 ± 4) % of the negative control whereas PEGylated chitosan/siRNA treated HCT-116 cells exhibited a reduction to approximately (72 ± 3) % of the negative control. Beta-catenin protein levels were normalized to vehicle control treated cells transfected with Lipofectamine/scrRNA (LF/scrRNA).

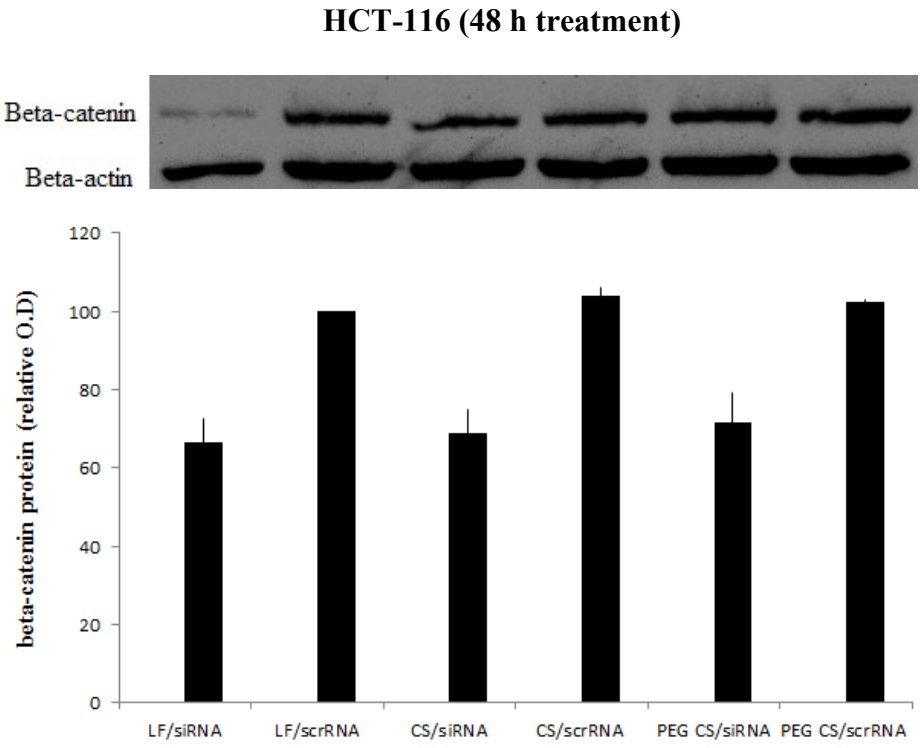

Figure 30. Chitosan/siRNA (CS siRNA) and PEGylated chitosan/siRNA (PEG CS/siRNA) treatments successfully reduced cellular beta-catenin protein level after 48 h. HCT-116 cells were plated and treated with 0.5 nanomoles per well of either siRNA or scrRNA encapsulated in either LF, CS or PEG CS for 48 h. Following treatment the proteins were harvested, electrophoresed and probed with beta-catenin and beta-actin antibodies as described in section 2.14. This experiment was performed three times with similar results; one representative western blot is shown for each time point. Below the western blot for each time point is a histogram with aligned bars that represent the percentage reduction in cellular beta-catenin protein level relative to beta actin for each blot. Values shown are the mean of three separate experiments ± SEM.

Figure 30 shows the results for HCT-116 cell transfected with (CS/siRNA) and (PEG CS/siRNA) or a corresponding negative control CS/scrRNA and PEG CS/scrRNA, after 48h. Lipofectamine/siRNA and Chitosan/siRNA treated cells exhibited a reduction in total cellular beta-catenin protein-levels to approximately (66 $\pm$ 6) % and (69 $\pm$ 6) % of the negative control whereas PEGylated chitosan/siRNA treated HCT-116 cells exhibited a reduction to approximately (72 $\pm$ 7) % of the negative control. Beta-catenin protein levels were normalized to vehicle control treated cells transfected with Lipofectamine/scrRNA (LF/scrRNA).

As seen in Figures 29 and 30 it can be concluded that the treatment with 0.5 nmol of siRNA successfully reduced beta-catenin protein level in HCT-116 cells and the transfection with CS/siRNA nanoparticles was more effective than with the PEG CS/siRNA nanoparticles. Even though the extant of PEGylation was minimized, PEG appears to produce a demonstrable effect on beta-catenin protein levels. We further conclude that the 48 h transfection with siRNA showed better results when compared to 24 h transfection with siRNA and this can be attributed to the time taken by the siRNA to effectively reduce the cellular beta-catenin protein levels.

CHAPTER IV

DISCUSSION

My discussion focuses on the following: (1) synthesis of chitosan/siRNA nanoparticles, (2) synthesis of PEGylated chitosan/siRNA nanoparticles, and (3) a comparison of beta-catenin reduction efficiency in cancer cells treated with Lipofectamine/siRNA, Chitosan/siRNA, and PEGylated chitosan/siRNA nanoparticles.

4.1 Chitosan Nanoparticles

The size of nanoparticles is very important because if the nanoparticles are too large then they cannot penetrate the cell. Depending upon the degree of deacetylation, chitosan has a natural tendency to aggregate thus increasing the overall size of a chitosan cluster. I adopted the ionic gelation method to reduce the aggregation of chitosan nanoparticles. For this purpose I added small amounts of TPP (a crosslinking agent) and siRNA to our chitosan solution. This was done to ensure that the maximum amount of negatively charged TPP and siRNA were available for the positively charged chitosan. The advantage in adopting this technique is formation of intramolecular binding of negatively charged siRNA to chitosan as opposed to intermolecular binding which would favor the formation of aggregates. I subsequently adopted a filtration technique to remove large aggregates. The approach appeared to be successful since the NP's were relatively small.

4.2 PEGylated Chitosan Nanoparticles

PEGylation of chitosan resulted in an increased solubility in aqueous solutions. We used methoxy poly (ethylene glycol) succinimidyl valerate instead of difunctional

poly (ethylene glycol) in order to avoid cross-linking of polymer strands. In this scenario, when the active group of mPEG reacts with the amino group of chitosan; the opposite end of the PEG is blocked with a methoxy group and cannot react with another amine of glucosamine. In the initial experiments the number of PEG attached per chitosan was 2.59 (2-3 PEG) but with time the mPEG-SVA hydrolyzed and the number of PEG attached per chitosan dropped to 0.125. The succinimide is fairly reactive and with time will hydrolyze when exposed to atmospheric moisture.

In the initial experiments, when we treated our cells with PEGylated chitosan/siRNA containing 0.1 nmol of siRNA, we achieved between 95 and 98% encapsulation efficiency. Unfortunately, there was no reduction in beta-catenin protein expression. In a second attempt we reacted the PEGylated chitosan in solution with four times as much siRNA, but the encapsulation efficiency decreased suggesting that a maximum amount of RNA had been encapsulated in the PEGylated chitosan nanoparticles. So we attempted another effort with our PEGylated chitosan nanoparticles wherein we added two times the siRNA than what was added in our first attempt. This time we achieved near 100% encapsulation efficiency and the amount of siRNA available for cell treatment was 0.5 nmol.

4.3 Beta-catenin Reduction

The total cellular beta-catenin in HCT-116 cells was evaluated at 24h and 48h after transfection. The transfection efficiencies were compared between Lipofectamine 2000, chitosan/siRNA nanoparticles and PEGylated chitosan/siRNA nanoparticles. Lipofectamine 2000 (positive control) is a cationic liposome and is highly toxic when used *in vivo*. Certain results showed that the delivery vectors were successful in reducing

the total cellular beta-catenin levels. As observed in the results, Lipofectamine/siRNA and Chitosan/siRNA nanoparticles had a better transfection efficiency and were able to reduce more cellular beta-catenin when compared to the PEGylated chitosan/siRNA nanoparticles. One reason which can be attributed to the underperformance of PEGylated chitosan/siRNA nanoparticles is that the number of PEG bonded to the chitosan in the final experiments was low (0.125 PEG per chitosan) and therefore not optimal. The question of whether PEGylated chitosan/siRNA nanoparticles can be more effective than non-PEGylated chitosan/siRNA nanoparticles still remains open and is subject to further research. The 48 h transfection period was adopted to check if we could further decrease the cellular beta-catenin levels. As seen from the results it can be concluded that the 48 h transfection with siRNA provided more satisfactory data when compared to the 24 h transfection with siRNA because of lower SEM values. Thus it can be stated that the siRNA takes 48 h to effectively down regulate the cellular protein levels. Nonetheless, our results indicate that chitosan/siRNA can be just as effective as Lipofectamine/ siRNA in reducing beta catenin protein expression. This is a very important result since Lipofectamine is toxic *in vivo* whereas chitosan is not.

REFERENCES

1. Aagaard, L.; Rossi, J. J. RNAi Therapeutics: Principles, Prospects and Challenges. *Adv. Drug Deliv. Rev.* **2007**, *59*, 75–86.
2. Alameh, M.; Dejesus, D.; Jean, M.; Darras, V.; Thibault, M.; Lavertu, M.; Buschmann, M. D.; Merzouki, A. Low Molecular Weight Chitosan Nanoparticulate System at Low N:P Ratio for Nontoxic Polynucleotide Delivery. *Int. J. Nanomedicine* **2012**, *7*, 1399–414
3. Akhtar, S.; Benter, I. Toxicogenomics of Non-Viral Drug Delivery Systems for RNAi: Potential Impact on siRNA-Mediated Gene Silencing Activity and Specificity. *Adv. Drug Deliv. Rev.* **2007**, *59*, 164–82.
4. Berthold, A.; Cremer, K.; Kreuter, J. Preparation and Characterization of Chitosan Microspheres as Drug Carrier for Prednisolone Sodium Phosphate as Model for Anti-Inflammatory Drugs. *J. Control. Release* **1996**, *39*, 17–25.
5. Casettari, L.; Vllasaliu, D.; Castagnino, E.; Stolnik, S.; Howdle, S.; Illum, L. PEGylated Chitosan Derivatives: Synthesis, Characterizations and Pharmaceutical Applications. *Prog. Polym. Sci.* **2012**, *37*, 659–685.
6. Cavallo, R.; Rubensteint, D.; Peifer, M. Armadillo and dTCF: a Marriage Made in the Nucleus. *Curr. Opin. Genet. Dev.* **1997**, *7*, 459–466
7. Chang, K.-L.; Higuchi, Y.; Kawakami, S.; Yamashita, F.; Hashida, M. Efficient Gene Transfection by Histidine-Modified Chitosan through Enhancement of Endosomal Escape. *Bioconjug. Chem.* **2010**, *21*, 1087–95.
8. Couzin, J. Breakthrough of the Year. Small RNAs Make Big Splash. *Science (80-.).* **2002**, *298*, 2296–2297.

9. Daniel, J. M.; Reynolds, A. B. Tyrosine Phosphorylation and Cadherin/catenin Function. *BioEssays* **1997**, *19*, 883–891.
10. De la Fuente, M.; Seijo, B.; Alonso, M. J. Novel Hyaluronic Acid-Chitosan Nanoparticles for Ocular Gene Therapy. *Invest. Ophthalmol. Vis. Sci.* **2008**, *49*, 2016–24.
11. Dillard, A. C.; Lane, M. A. Retinol Decreases b -Catenin Protein Levels in Retinoic Acid-Resistant Colon Cancer Cell Lines. 2007, 329, 315–329.
12. Filion, M. C.; Phillips, N. C. Major Limitations in the Use of Cationic Liposomes for DNA Delivery. *Int. J. Pharm.* **1998**, *162*, 159–170.
13. Fire, A.; Xu, S.; Montgomery, M. K.; Kostas, S. A.; Driver, S. E.; Mello, C. C. Potent and Specific Genetic Interference by Double-Stranded RNA in Caenorhabditis Elegans. *Nature* **1998**, *391*, 806–811.
14. Garcia-Fuentes, M.; Alonso, M. J. Chitosan-Based Drug Nanocarriers: Where Do We Stand? *J. Control. Release* **2012**, *161*, 496–504.
15. Goldstein, M. J.; Mitchell, E. P. Carcinoembryonic Antigen in the Staging and Follow-up of Patients with Colorectal Cancer. **2005**, *23*, 338–351.
16. Gorzelanny, C.; Pöppelmann, B.; Pappelbaum, K.; Moerschbacher, B. M.; Schneider, S. W. Human Macrophage Activation Triggered by Chitotriosidase-Mediated Chitin and Chitosan Degradation. *Biomaterials* **2010**, *31*, 8556–8563.
17. He, P.; Davis, S. S.; Illum, L. In Vitro Evaluation of the Mucoadhesive Properties of Chitosan Microspheres. *Int. J. Pharm.* **1998**, *166*, 75–88.

18. He, X.; Saint-Jeannet, J. P.; Woodgett, J. R.; Varmus, H. E.; Dawid, I. B. Glycogen Synthase Kinase-3 and Dorsoventral Patterning in Xenopus Embryos. *Nature* **1995**, *374*, 617–622.

19. Illum, L. Nasal Drug Delivery: New Developments and Strategies. *Drug Discov. Today* **2002**, *7*, 1184–9.

20. Illum, L. Chitosan and Its Use as a Pharmaceutical Excipient. *Pharm. Res.* **1998**, *15*, 1326–1331

21. Jeong, Y.-I.; Kim, D.-G.; Jang, M.-K.; Nah, J.-W. Preparation and Spectroscopic Characterization of Methoxy Poly(ethylene Glycol)-Grafted Water-Soluble Chitosan. *Carbohydr. Res.* **2008**, *343*, 282–9.

22. Jere, D.; Jiang, H.-L.; Kim, Y.-K.; Arote, R.; Choi, Y.-J.; Yun, C.-H.; Cho, M.-H.; Cho, C.-S. Chitosan-Graft-Polyethylenimine for Akt1 siRNA Delivery to Lung Cancer Cells. *Int. J. Pharm.* **2009a**, *378*, 194–200.

23. Jere, D.; Jiang, H. L.; Arote, R.; Kim, Y. K.; Choi, Y. J.; Cho, M. H.; Akaike, T.; Cho, C. S. Degradable Polyethylenimines as DNA and Small Interfering RNA Carriers. *Expert Opin. Drug Deliv.* **2009b**, *6*, 827–834.

24. Ji, A. M.; Su, D.; Che, O.; Li, W. S.; Sun, L.; Zhang, Z. Y.; Yang, B.; Xu, F. Functional Gene Silencing Mediated by chitosan/siRNA Nanocomplexes. *Nanotechnology* **2009**, *20*, 405103.

25. Kato, Y.; Onishi, H.; Machida, Y. Contribution of Chitosan and Its Derivatives to Cancer Chemotherapy. **2005**, *310*, 301–310.

26. Lavertu, M.; Xia, Z.; Serreqi, a. N.; Berrada, M.; Rodrigues, a.; Wang, D.; Buschmann, M. D.; Gupta, A. A Validated 1H NMR Method for the Determination of the Degree of Deacetylation of Chitosan. *J. Pharm. Biomed. Anal.* **2003**, *32*, 1149–1158.

27. Lee, D. W.; Yun, K.-S.; Ban, H.-S.; Choe, W.; Lee, S. K.; Lee, K. Y. Preparation and Characterization of Chitosan/polyguluronate Nanoparticles for siRNA Delivery. *J. Control. Release* **2009**, *139*, 146–52.

28. Lee, E.; Kim, H.; Lee, I.-H.; Jon, S. In Vivo Antitumor Effects of Chitosan-Conjugated Docetaxel after Oral Administration. *J. Control. Release* **2009**, *140*, 79–85.

29. Lehr, C. M.; Bouwstra, J. A.; Schacht, E. H.; Junginger, H. E. In Vitro Evaluation of Mucoadhesive Properties of Chitosan and Some Other Natural Polymers. *Int. J. Pharm.* **1992**, *78*, 43–48.

30. Leong, K. W.; Mao, H. Q.; Truong-Le, V. L.; Roy, K.; Walsh, S. M.; August, J. T. DNA-Polycation Nanospheres as Non-Viral Gene Delivery Vehicles. *J. Control. Release* **1998**, *53*, 183–193.

31. Li, X.; Zhang, Y.; Kang, H.; Liu, W.; Liu, P.; Zhang, J.; Harris, S. E.; Wu, D. Sclerostin Binds to LRP5/6 and Antagonizes Canonical Wnt Signaling. *J. Biol. Chem.* **2005**, *280*, 19883–7.

32. Liu, F.; Huang, L. Development of Non-Viral Vectors for Systemic Gene Delivery. *J. Control. Release* **2002**, *78*, 259–66.

33. Malhotra, M.; Lane, C.; Tomaro-Duchesneau, C.; Saha, S.; Prakash, S. A Novel Method for Synthesizing PEGylated Chitosan Nanoparticles: Strategy, Preparation, and in Vitro Analysis. *Int. J. Nanomedicine* **2011**, *6*, 485–94.

34. Mansouri, S.; Lavigne, P.; Corsi, K.; Benderdour, M.; Beaumont, E.; Fernandes, J. C. Chitosan-DNA Nanoparticles as Non-Viral Vectors in Gene Therapy: Strategies to Improve Transfection Efficacy. *Eur. J. Pharm. Biopharm.* **2004**, *57*, 1–8.

35. Murugadoss, A; Chattopadhyay, A. A "Green" Chitosan-Silver Nanoparticle Composite as a Heterogeneous as Well as Micro-Heterogeneous Catalyst. *Nanotechnology* **2008**, *19*, 015603.

36. Muzzarelli, R. A. A.; Muzzarelli, C. Chitosan Chemistry: Relevance to the Biomedicine Sciences. *Adv. Polym. Sci.* **2005**, *186*, 151–209.

37. Oligino, T. J.; Yao, Q.; Ghivizzani, S. C.; Robbins, P. Vector Systems for Gene Transfer to Joints. *Clin. Orthop. Relat. Res.* **2000**, S17–S30.

38. Orsulic, S.; Huber, O.; Aberle, H.; Arnold, S.; Kemler, R. E-Cadherin Binding Prevents Beta-Catenin Nuclear Localization and Beta-catenin/LEF-1-Mediated Transactivation. *J. Cell Sci.* **1999**, *112 (Pt 8*, 1237–1245.

39. Pack, D. W.; Hoffman, A. S.; Pun, S.; Stayton, P. S. Design and Development of Polymers for Gene Delivery. *Nat Rev Drug Discov* **2005**, *4*, 581–593.

40. Pai, L. M.; Orsulic, S.; Bejsovec, A.; Peifer, M. Negative Regulation of Armadillo, a Wingless Effector in Drosophila. *Development* **1997**, *124*, 2255–2266.

41. Papkoff, J.; Rubinfeld, B.; Schryver, B.; Polakis, P. Wnt-1 Regulates Free Pools of Catenins and Stabilizes APC-Catenin Complexes . *Mol. Cell. Biol.* **1996**, *16*, 2128–2134.

42. Peifer, M.; Sweeton, D.; Casey, M.; Wieschaus, E. Wingless Signal and Zeste-White 3 Kinase Trigger Opposing Changes in the Intracellular Distribution of Armadillo. *Dev. Cambridge Engl.* **1994**, *120*, 369–380.

43. Prego, C.; Torres, D.; Fernandez-Megia, E.; Novoa-Carballal, R.; Quiñoá, E.; Alonso, M. J. Chitosan-PEG Nanocapsules as New Carriers for Oral Peptide Delivery. Effect of Chitosan Pegylation Degree. *J. Control. Release* **2006**, *111*, 299–308.

44. Raviña, M.; Cubillo, E.; Olmeda, D.; Novoa-Carballal, R.; Fernandez-Megia, E.; Riguera, R.; Sánchez, A.; Cano, A.; Alonso, M. J. Hyaluronic Acid/chitosan-g-Poly(ethylene Glycol) Nanoparticles for Gene Therapy: An Application for pDNA and siRNA Delivery. *Pharm. Res.* **2010**, *27*, 2544–55.

45. Rudzinski, W. E.; Aminabhavi, T. M. Chitosan as a Carrier for Targeted Delivery of Small Interfering RNA. *Int. J. Pharm.* **2010**, *399*, 1–11.

46. Siegel, R.; Naishadham, D.; Jemal, A. Cancer Statistics , 2013, Ca-a Cancer Journal for Clinicians,. **2013**, *63*, 11–30.

47. Smith, J.; Wood, E.; Dornish, M. Effect of Chitosan on Epithelial Cell Tight Junctions. *Pharm. Res.* **2004**, *21*, 43–9.

48. Strand, S. P.; Issa, M. M.; Christensen, B. E.; Vårum, K. M.; Artursson, P. Tailoring of Chitosans for Gene Delivery: Novel Self-Branched Glycosylated Chitosan Oligomers with Improved Functional Properties. *Biomacromolecules* **2008**, *9*, 3268–3276.

49. Teijeiro-Osorio, D.; Remuñán-López, C.; Alonso, M. J. Chitosan/cyclodextrin Nanoparticles Can Efficiently Transfect the Airway Epithelium in Vitro. *Eur. J. Pharm. Biopharm. Off. J. Arbeitsgemeinschaft fur Pharm. Verfahrenstechnik eV* **2009**, *71*, 257–263.

50. Wheeler, J. J.; Palmer, L.; Ossanlou, M.; MacLachlan, I.; Graham, R. W.; Zhang, Y. P.; Hope, M. J.; Scherrer, P.; Cullis, P. R. Stabilized Plasmid-Lipid Particles: Construction and Characterization. *Gene Ther.* **1999**, *6*, 271–81.

51. Xu, Y.; Wen, Z.; Xu, Z. Chitosan Nanoparticles Inhibit the Growth of Human Hepatocellular Carcinoma Xenografts through an Antiangiogenic Mechanism. *Anticancer Res.* **2009**, *29*, 5103–9.

52. Yost, C.; Torres, M.; Miller, J. R.; Huang, E.; Kimelman, D.; Moon, R. T. The Axis-Inducing Activity, Stability, and Subcellular Distribution of Beta-Catenin Is Regulated in Xenopus Embryos by Glycogen Synthase Kinase 3. *Genes Dev.* **1996**, *10*, 1443–1454.